Valparaiso University
ValpoScholar

Physics and Astronomy Faculty Publications | Department of Physics and Astronomy

7-27-2000

Trajectory mapping: A tool for validation of trace gas observations

Gary A. Morris
Valparaiso University, gary.morris@valpo.edu

James F. Gleason
NASA Goddard Space Flight Center, Greenbelt, MD

Jerald Ziemke
Software Corporation of America

Mark R. Schoeberl
Earth Sciences Division, NASA Goddard Space Flight Center, Greenbelt, MD

Follow this and additional works at: http://scholar.valpo.edu/phys_astro_fac_pub

 Part of the Atmospheric Sciences Commons

Recommended Citation
Morris, G. A., J. F. Gleason, J. Ziemke, and M. R. Schoeberl (2000), Trajectory mapping: A tool for validation of trace gas observations, J. Geophys. Res., 105(D14), 17,875–17,894, doi:10.1029/1999JD901118.

This Article is brought to you for free and open access by the Department of Physics and Astronomy at ValpoScholar. It has been accepted for inclusion in Physics and Astronomy Faculty Publications by an authorized administrator of ValpoScholar. For more information, please contact a ValpoScholar staff member at scholar@valpo.edu.

JOURNAL OF GEOPHYSICAL RESEARCH, VOL. 105, NO. D14, PAGES 17,875–17,894, JULY 27, 2000

Trajectory mapping: A tool for validation of trace gas observations

Gary A. Morris,[1] James F. Gleason,[2] Jerald Ziemke,[3] and Mark R. Schoeberl[2]

Abstract. We investigate the effectiveness of trajectory mapping (TM) as a data validation tool. TM combines a dynamical model of the atmosphere with trace gas observations to provide more statistically robust estimates of instrument performance over much broader geographic areas than traditional techniques are able to provide. We present four detailed case studies selected so that the traditional techniques are expected to work well. In each case the TM results are equivalent to or improve upon the measurement comparisons performed with traditional approaches. The TM results are statistically more robust than those achieved using traditional approaches since the TM comparisons occur over a much larger range of geophysical variability. In the first case study we compare ozone data from the Halogen Occultation Experiment (HALOE) with Microwave Limb Sounder (MLS). TM comparisons appear to introduce little to no error as compared to the traditional approach. In the second case study we compare ozone data from HALOE with that from the Stratospheric Aerosol and Gas Experiment II (SAGE II). TM results in differences of less than 5% as compared to the traditional approach at altitudes between 18 and 25 km and less than 10% at altitudes between 25 and 40 km. In the third case study we show that ozone profiles generated from HALOE data using TM compare well with profiles from five European ozonesondes. In the fourth case study we evaluate the precision of MLS H_2O using TM and find typical precision uncertainties of 3–7% at most latitudes and altitudes. The TM results agree well with previous estimates but are the result of a global analysis of the data rather than an analysis in the limited latitude bands in which traditional approaches work. Finally, sensitivity studies using the MLS H_2O data show the following: (1) a combination of forward and backward trajectory calculations minimize uncertainties in isentropic TM; (2) although the uncertainty of the technique increases with trajectory duration, TM calculations of up to 14 days can provide reliable information for use in data validation studies; (3) a correlation coincidence criterion of 400 km produces the best TM results under most circumstances; (4) TM performs well compared to (and sometimes better than) traditional approaches at all latitudes and in most seasons; and (5) TM introduces no statistically significant biases at altitudes between 22 and 40 km.

1. Introduction

An important part of the scientific method is establishing the reliability of experimental data. Many instruments can be calibrated in the laboratory both before and after making measurements, providing an accurate assessment of changes in the instrument's performance over the observation period. For example, one of the most extensive validation studies to date is the Balloon Ozone Intercomparison Campaign (BOIC) [*Hilsenrath et al.*, 1986]. During this campaign a suite of instruments designed to measure ozone were calibrated in the laboratory, gathered to fly on the same balloon payload, and then recalibrated in the laboratory after flight. The campaign provided some of the most thorough assessments of ozone measurement quality to date.

Unfortunately, such thorough studies cannot be feasibly performed for instruments in space. While careful evaluation of instrument performance can take place in the laboratory before launch, evaluation generally cannot be conducted in the laboratory after launch, the shuttle solar backscatter ultraviolet (SSBUV) instrument being a notable exception [*Hilsenrath et al.*, 1993].

Most satellite instruments utilize some type of calibration, either viewing an internal source (like a blackbody) or an external source (like the Sun or cold space). For example, the Cryogenic Limb Array Etalon Spectrometer (CLAES) closed its doors once a month to view a stable, known blackbody source for calibration purposes [*Roche et al.*, 1993], and the Improved Stratospheric and Mesospheric Sounder (ISAMS) carried on board an internal calibration target [*Rodgers et al.*, 1996] as well as cells containing the target trace gas species for use in the pressure modulator radiometry technique [*Taylor*, 1983; *Taylor, et al.*, 1993]. While such instruments provide an internal consistency check on the data, the problem of external calibration remains. Most measurements from space are forced to rely upon indirect determinations of instrument performance.

Although satellite instruments pose substantial challenges to the evaluation of their performance, they do provide significant advantages over their in situ counterparts. Satellite instruments are capable of providing global coverage, including measurements over remote regions. Little in situ data is returned over the

[1] Department of Physics and Astronomy, Valparaiso University, Valparaiso, Indiana.
[2] Laboratory for Atmospheres, NASA Goddard Space Flight Center, Greenbelt, Maryland.
[3] Software Corporation of America, Greenbelt, Maryland.

Copyright 2000 by the American Geophysical Union.

Paper number 1999JD901118.
0148-0227/00/1999JD901118$09.00

oceans or in the Southern Hemisphere, owing to the sparse distribution of ground stations. In addition, in situ data sets are likely to be quite limited temporally. For example, ozonesondes provide high-resolution profiles of ozone but are typically launched only a few times a month. Satellite instruments tend to provide lower spatial resolution than in situ measurements do but can achieve a wide range of spatial and temporal resolutions depending upon the instrument type and satellite orbit. The geographic and temporal advantages of satellite instruments compliment the high spatial resolution of in situ measurements. Overcoming the validation issues associated with satellite measurements therefore becomes an essential task in producing a valuable, reliable data set.

The use of trajectory calculations in interpreting satellite data has become increasingly popular over the last several years. The technique was first applied to map the sparse Halogen Occultation Experiment (HALOE) data set, expanding the coverage provided by the solar occultation instrument [*Pierce et al.*, 1994]. *Morris et al.* [1995] applied the technique to mapping data from the Microwave Limb Sounder (MLS) and CLAES. Neither of these studies, however, produced uniformly gridded data. *Sutton et al.* [1994], *Newman and Schoeberl* [1995], and *Schoeberl and Newman* [1995] all developed the reverse-domain-filling (RDF) to create uniformly gridded maps of satellite data by initializing trajectories on a uniform grid and then assigning constituent values to the grid points using back trajectory encounters with satellite observations. Trajectory calculations have also been frequently used in chemical box model calculations [*Kawa et al.*, 1993; *Morris et al.*, 1998] and to infer chemical loss of ozone during the Arctic winter season [*Manney et al.*, 1995; *Rex et al.*, 1998]. Given their widespread application, it is important to develop a better understanding of the limitations of trajectory calculations and the magnitudes of the errors they introduce in order to correctly interpret the results of such studies.

In this paper, we investigate the trajectory-mapping (TM) technique for use in evaluating satellite instrument performance. We divide the paper into three parts. In section 2, we examine the use of TM in studies designed to assess the accuracy of satellite observations. In section 3 we examine the use of TM in studies designed to evaluate the precision of satellite observations. Finally, in section 4 we present sensitivity studies that investigate the impact on results achieved using TM of changes in trajectory calculation duration, correlation criteria, latitude, altitude, and season.

2. Accuracy Assessment: The Problems of Comparing Two Data Sets

In this section we review previous approaches to the problem of assessing satellite instrument accuracy postlaunch. We then describe the application of TM to the problem and apply the technique to three case studies: a comparison of HALOE and MLS ozone data, a comparison of HALOE and Stratospheric Aerosol and Gas Experiment II (SAGE II) ozone data, and a comparison of HALOE ozone data with ozonesondes.

2.1. Traditional Approaches

In sections 2.1.1 and 2.1.2 we review previous efforts to assess instrument performance using rare coincidences between observations from two different instruments or using zonal means of the data from two different instruments. We will refer to these two approaches to data validation as "traditional" approaches.

2.1.1. Coincident comparisons. A number of strategies have been designed in an attempt to validate satellite data. Previous assessments of instrument accuracy have utilized comparisons of satellite observations with correlative measurements from radiosondes [*Rind et al.*, 1993], balloons [*Russell et al.*, 1996a; *Veiga et al.*, 1995], rockets [*Roche et al.*, 1996], space shuttle instruments [*Kumer et al.*, 1996], ground-based microwave radiometer measurements [*Conner et al.*, 1996], other satellite instruments [*Cunnold et al.*, 1996], and lidar [*Singh et al*, 1996; *Bailey, et al.*, 1996]. In each case, correlation criteria are established to define "coincident" observations as those made within a specified distance and time of one another. Spatial separations are typically hundreds of kilometers while the time between such measurements can range from minutes to days or longer. Atmospheric changes occurring on smaller spatial and temporal scales often result in apparent disagreements between the data. As one example, *McDermid et al.* [1990] attempt to use a variety of ground-based measurement techniques to help validate SAGE II ozone measurements. Out of the three coincident cases shown, only one demonstrates good agreement. The authors attribute the disagreements observed in the other two cases to meteorology in order to discard them, and then the authors conclude that the SAGE II ozone agrees with the ground measurements to within 5%. Clearly, additional coincidences or a more thorough analysis of the meteorology would enhance our confidence in such conclusions.

2.1.2. Zonal means. Another technique for evaluating satellite accuracy involves the comparison of zonal means. Zonal mean satellite data have been compared to gridded meteorological analyses [*Gille et al.*, 1996], other satellite instruments [*Remedios et al.*, 1996], and model results [*Lopez-Valverde et al.*, 1996; *Nightingale et al.*, 1996]. While more statistically satisfying than coincidence studies, zonal mean analyses have their own shortcomings. First, longitudinal gradients are lost in the zonal averaging. Second, in some cases the temporal difference between the measurements used to compile the zonal average maps is quite large. Third, the comparisons of zonal mean data are limited to specific latitudes.

Solar occultation instruments such as SAGE II and HALOE can only make their observations in two latitude bands each day. Over the course of 10-15 days the instruments will sweep across most latitudes. The sparse nature of such data sets virtually requires the use of zonal mean comparisons for data validation purposes. *Conner et al.* [1996] compared zonal mean SAGE II measurements (1986–1990) and Limb Infrared Monitor of the Stratosphere (LIMS, 1979) ozone measurements with those of ISAMS (1992). Clearly, substantial differences between the data sets exist owing solely to the real atmospheric differences between the observation periods of 1979, the late 1980s, and 1992. Similarly, *Russell et al.* [1993] compared zonal mean HALOE measurements from May 1992 with measurements of the same constituents made by the Atmospheric Trace Molecule Spectroscopy Experiment (ATMOS) in May 1985, a full 7 years earlier. In addition to the large temporal separation, the data were separated in latitude by 5°. While in each case the authors were only trying to demonstrate qualitative confirmation of the newer measurements, the value of such comparisons is clearly limited. Finally, we must be aware that the HALOE latitude/pressure plots, such as those found in the work of *Russell et al.* [1996b], are not synoptic: their production requires at least 2 weeks of observations, with each latitude observed on a different day.

This paper explores the effectiveness of an alternative method for evaluating postlaunch instrument performance. Using the trajectory-mapping technique [*Morris et al.*, 1995], we can assess the quality of satellite data at a wider range of latitudes and times than that assessed by previous techniques. After reviewing the trajectory-mapping (TM) technique, we apply it to three case studies.

In the first case we compare HALOE and MLS ozone measurements. MLS itself passively observes microwave emissions

from the limb of the atmosphere. MLS observations have a vertical resolution of ~6 km and a horizontal resolution of ~400 km × 400 km. Since MLS is a limb emission instrument, it provides relatively good coverage (>1300 measurements) on a daily basis. The probability of coincidences using traditional techniques is relatively high in such a case, so we expect the traditional methods outlined above to perform well. The comparison of HALOE and MLS ozone measurements therefore provides a test case to evaluate the magnitude of the errors introduced by TM. Our results indicate that TM increases the number of coincidences as compared to the traditional approach without negatively affecting the uncertainty of the comparisons.

In the second case we compare HALOE and SAGE II ozone. Since both instruments are solar occultation instruments, the two data sets are quite sparse. The nature of these data sets makes comparisons using traditional techniques difficult. We demonstrate that TM substantially increases the number of coincidences between the two satellite instruments and expands the latitude range of coincidences beyond traditional techniques. Furthermore, by taking into account dynamical variability, the trajectory technique often improves the statistics of coincident comparisons relative to more traditional approaches. We also demonstrate that the impact of the length of the trajectory calculations on the uncertainty of the comparisons is relatively small for calculations of up to 2 weeks and that the use of combined forward and backward calculations tends to minimize errors incurred through the trajectory technique (a more detailed examination of these subjects can be found in section 4.1).

In the third case we compare HALOE ozone observations to measurements provided by ozonesondes at five European stations. We demonstrate that TM provides an appropriate and reliable approach to comparing observations made by instruments of highly different character: satellite observations from space and in situ observations from balloons. This comparison highlights the advantages provided by TM over traditional validation techniques.

2.1.3. Review of the trajectory-mapping technique. In brief, TM takes advantage of quasi-conserved quantities following air parcel motion, namely the mixing ratio and potential temperature. Several authors have noted that the latter of these is reasonably well conserved along air parcel trajectories for 5–10 days [*Schoeberl and Sparling*, 1994; *Sutton et al.*, 1994; *Morris et al.*, 1995]. The technique was first applied to satellite data by *Pierce et al.* [1994]. To create a synoptic trajectory map from satellite data, we initialize an air parcel in our model at the time and location of each satellite observation. The model then isentropically advects these air parcels forward or backward in time to the time at which we desire an output synoptic map. By including several days of observations and using a combination of forward and backward calculations, we greatly enhance the density of coverage in our trajectory maps. Furthermore, by accounting for dynamical changes in the atmosphere between observation times, TM provides better representations of the measured constituent fields than those from asynoptic schemes. TM can be straightforwardly applied to the validation of data and the production of synoptic maps, as outlined below and demonstrated in our case studies. For all the studies presented in this paper, we use the trajectory model of *Schoeberl and Sparling* [1994].

To compare data from two instruments, we first create a series of synoptic trajectory maps from one of the data sets (generally, the instrument that provides better coverage). We then sample the synoptic maps created from the first instrument at the times and locations of the observations of the second instrument. We consider those trajectory-mapped measurements appearing within a specified distance of the observations of the second instrument to be coincident. A maximum time difference between the observations can also be specified to limit the duration of trajectory calculations.

Ideally, we would create a trajectory map at the time of each new observation by the second instrument. In so doing, we account for movement of air parcels in which the first instrument made its observations. Because of the number of observations satellites make daily, however, this practice becomes somewhat impractical, even for solar occultation instruments, which record 30 observations per day. Instead, we produce trajectory maps twice per day using data from both instruments, at midnight and noon Universal time (UT). All the new observations from the second instrument appearing in a given trajectory map are then compared with the surrounding, trajectory-mapped measurements from the first instrument. Observations from the second instrument are thus advected for less than 12 hours by the model. *Morris et al.* [1995] demonstrate that advection over such short timescales should have little impact on our calculations. This procedure can be applied to comparisons of a wide variety of data sets, including aircraft, satellite, and balloons.

Morris et al. [1995] have previously outlined and demonstrated this technique for data validation in a comparison of water vapor data from the Halogen Occultation Experiment (HALOE) and the Microwave Limb Sounder (MLS) aboard the Upper Atmosphere Research Satellite (UARS). In sections 2.2–2.4 we more rigorously and quantitatively evaluate the effectiveness of the technique in validating ozone profiles by estimating the magnitude of the uncertainties introduced when employing the TM technique. To evaluate the uncertainty inherent in the technique itself, we compare the results achieved through TM with those achieved using the traditional approaches under circumstances in which the traditional approach is expected to perform well. Observed differences in the results may then be mainly attributed to the use of TM in performing the comparisons.

2.2. Case Study 1: HALOE Versus MLS Ozone

We have applied the TM technique to the problem of comparing HALOE (Version 18) and MLS (Version 4) ozone measurements during the 8-day period, September 23–30, 1996. MLS provides a relatively dense data set containing ~1300 measurements per day. HALOE provides ~30 observations per day, evenly divided between the two latitude bands in which the solar occultations occur. The relatively high density of the MLS observations should permit traditional validation techniques to perform well. Therefore, comparing the results achieved with TM to the traditional results, we can derive an estimate of the uncertainties introduced by TM. MLS data below 46 hPa were excluded from this study as per the recommendation of *Froidevaux et al.* [1996].

Figure 1 shows a scatterplot of MLS observations made within 12 hours of and within 400 km of HALOE observations against those HALOE observations for data on the 800 K (~30 km) potential temperature surface. The results shown in Figure 1 therefore represent the type of results that a traditional, coincident data validation approach can achieve.

Next, we apply TM to the same data validation problem. Each MLS measurement was initialized as a single parcel in the trajectory model and then advected forward and backward in time for 1.5 days using analyzed wind fields from the U.K. Meteorological Office (UKMO). The MLS trajectory maps were then sampled using the HALOE observation pattern. Those MLS observations advected to within 400 km of the new HALOE observations are considered to be coincident. We choose a coincidence criterion of 400 km because this distance is approximately the size of the MLS observation footprint and this magnitude coincidence criterion appears to minimize uncertainties in TM, as

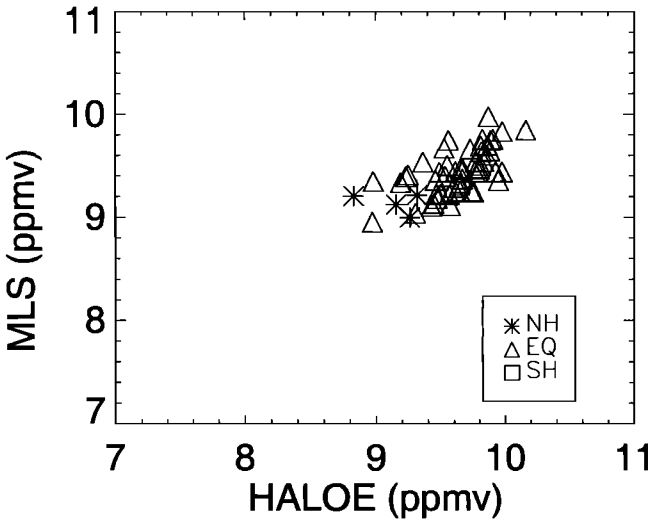

Figure 1. Microwave Limb Sounder (MLS) versus Halogen Occultation Experiment (HALOE) using traditional coincidence criteria of 400 km separation and 12 hour maximum time difference for ozone data gathered on the 800 K potential temperature surface (~30 km) during September 23–30, 1996. NH indicates coincidences in the Northern Hemisphere (20°–90°N), EQ indicates coincidences in the equatorial region (20°S–20°N); and SH indicates coincidences in the Southern Hemisphere (20°–90°S).

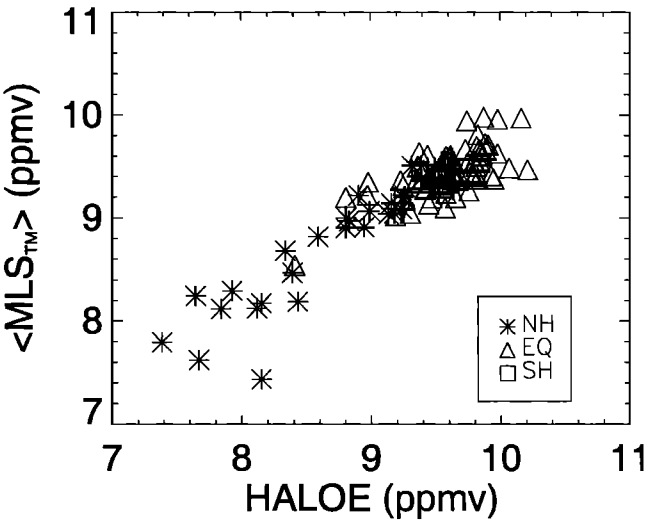

Figure 2. As in Figure 1, MLS versus HALOE, but using the trajectory-mapping (TM) approach. Trajectory calculations are limited to 1.5-day duration. Advected MLS measurements within 400 km of the Stratospheric Aerosol and Gas Experiment II (SAGE II) observations are considered coincident.

shown by the sensitivity study in section 4.2. The average of the nearby MLS observations is then compared with the HALOE observations. Figure 2 shows a scatterplot of the trajectory-mapped MLS ozone versus the HALOE observations on the 800 K (~30 km) potential temperature surface. The trajectory technique has increased the number of coincidences between the two data sets providing coincidences at locations inaccessible to the traditional technique.

As a measure of the quality of the two techniques, we compute the root-mean-square (RMS) difference between the HALOE and MLS data sets. We define RMS to be

$$\mathrm{RMS}=\sqrt{\sum_{i=1}^{N}\frac{\bar{y}_i-x_i}{Nx_i}},$$

where the $\bar{y}_i$ are the average of the trajectory-mapped MLS observations in the vicinity of the HALOE measurement (x_i) and N is the total number of HALOE measurements that can be validated. For HALOE-MLS water vapor comparison at this altitude, the RMS statistic shows a slight increase for the trajectory technique (3.4%) relative to the traditional technique (3.0%).

We repeat this study at six vertical levels between 550 K (~23 km) and 1200 K (~40 km). Table 1 summarizes the RMS differences between the data sets. The data show that TM substantially increases the number of coincidences over the traditional approach. In particular, TM provides coincidences in the Southern Hemisphere, where traditional techniques cannot.

The data in Table 1 suggest that TM does not significantly increase or decrease the uncertainty as compared to the traditional technique. This result is not surprising given that MLS makes more than 1300 measurements each day. The spatial and temporal differences between MLS and HALOE measurements are likely to be relatively small. As a result, the penalty incurred for not accounting for the dynamics in the MLS-HALOE comparisons is not large, and the traditional approach produces satisfactory results. Nevertheless, the significant increase in correlated observations between MLS and HALOE through the use of trajectory techniques provides an incentive for their use in this case as well. In particular, the geographic area over which intercomparisons of the data can be made is expanded through the use of the TM technique. We believe this geographic advantage of TM over the traditional approach warrants its use even in cases for

Table 1. Root-Mean-Square Statistic and Number of Coincidences in the Southern Hemisphere, Equatorial Region, and Northern Hemisphere for HALOE–MLS Intercomparisons

	1.5-Day Trajectory Mapping				Traditional Approach			
Theta, K	RMS, %	SH	EQ	NH	RMS, %	SH	EQ	NH
550	14.0	6	65	21	13.5	0	53	4
600	5.8	5	68	22	6.1	0	53	4
700	7.2	5	71	23	7.2	0	53	4
800	3.4	5	73	26	3.0	0	53	4
1000	3.4	6	73	23	3.6	0	53	4
1200	5.4	6	68	24	4.5	0	53	4

See text for definition of RMS statistic. Southern Hemisphere (SH) is 20°–90°S, equatorial region (EQ) is 20°S–20°N, and Northern Hemisphere (NH) is 20°–90°N). HALOE, Halogen Occultation Experiment; MLS, Microwave Limb Sounder.

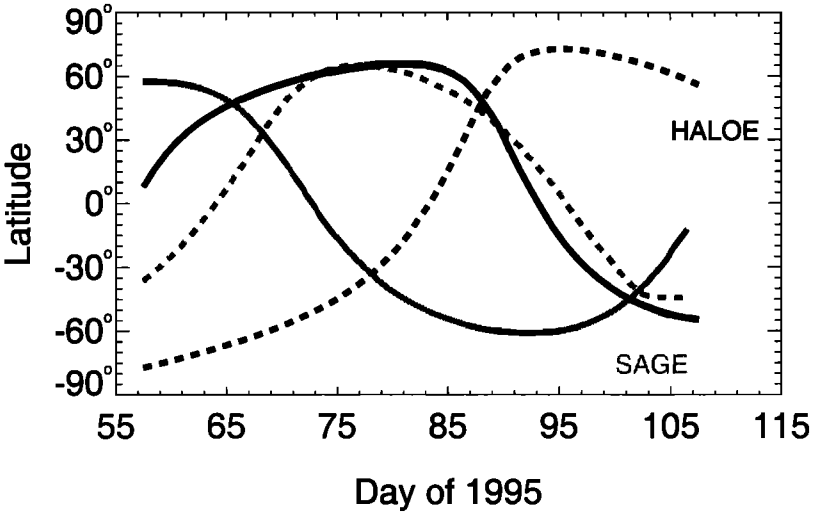

Figure 3. The latitudes at which HALOE and SAGE II make their observations between February 26 and April 19, 1995. We examine those close coincidences that occur around 60°N and 35°S on March 19 (day 78) in this study. The dark lines denote SAGE II observation latitudes while the light lines denote HALOE observation latitudes. The dashed lines indicate sunrise observations while the solid lines indicate sunset observations.

which the traditional approaches work well. Traditional approaches must extrapolate results achieved at a single latitude or over a limited range of latitudes to global data sets. Agreements between the data sets at one latitude, however, do not necessarily indicate a global agreement between the data sets. TM therefore can better provide validation as a function of latitude than can traditional techniques.

We also note from the data in Table 1 that the disagreements between the data sets appear largest at the lower altitudes, decrease through a minimum around 800 K, and then increase again above 800 K. The increase above 800 K is likely due to the diminishing validity of the conservation assumptions in the trajectory technique (discussed further in case study 2 in section 2.3). Increases in uncertainties below 800 K are consistent with validation work on the MLS ozone data reported by *Froidevaux et al.* [1996].

2.3. Case Study 2: HALOE Versus SAGE II Ozone

A more difficult challenge to traditional validation techniques is presented by attempts to compare two sparse data sets. We now compare SAGE II (version 5.93) and HALOE (version18) ozone measurements from February 26 to April 19, 1995, hereinafter referred to as the March 1995 period. Figure 3 shows the HALOE and SAGE II data-gathering pattern for this time period. We note that for most of this time period, HALOE and SAGE II are making measurements at different geographic locations. During four periods, however, they are measuring at the same latitude on the same days: March 6 (day 65), March 12–22 (days 71–81), March 28–31 (days 87–90), and April 11 (day 101). Over the HALOE and SAGE II data records, the number of coincidences observed during this time period is relatively large, which makes this period a best–case scenario for using traditional validation techniques to compare two data sets. For most of the record, HALOE and SAGE II do not often make measurements in the same latitude bands at the same time.

2.3.1. Traditional approaches: Coincident comparisons. When HALOE and SAGE II retrieve ozone in the same latitude bands, the traditional coincidence approach enjoys its greatest chance of success. Figure 4 shows a scatterplot of the coincident ozone measurements retrieved by HALOE and SAGE II at the 800 K level over the entire March 1995 period. If we consider HALOE and SAGE II to be coincident when the HALOE measurement is made within 400 km and 12 hours of the SAGE II observation, we find 151 coincidences (a stricter time criteria of 10 hours limits the number of coincidences to just eight). Therefore roughly 10% of the 1500 measurements made by each HALOE and SAGE II over our study period can be correlated in this way.

Furthermore, the coincident approach can only comment on the relationship between the two instruments in the restricted latitude bands of concurrent observation. Figure 5 depicts the number of coincidences between HALOE and SAGE II observations as a function of latitude in 5° latitude bins. The starred line in Figure 5 represents the traditional approach. Traditional comparisons in the Northern Hemisphere (Figure 5a) are basically restricted to a 15° latitude band around 60°N. Only six observations satisfy the coincidence criteria in the Southern Hemisphere (Figure 5b) during the entire study period. Such infrequent coincidences hamper validation efforts. The temporal differences between and sparse nature of the two data sets virtu-

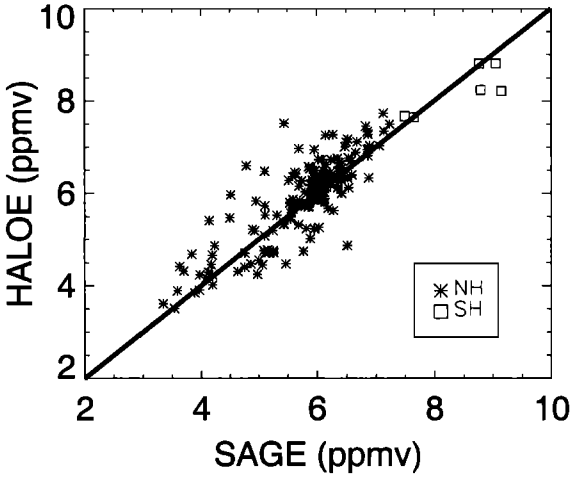

Figure 4. HALOE versus SAGE II ozone using traditional coincidence criteria of 400 km separation and 12 hour maximum time difference for data gathered on the 800 K potential temperature surface during the period February 26 through April 19, 1995.

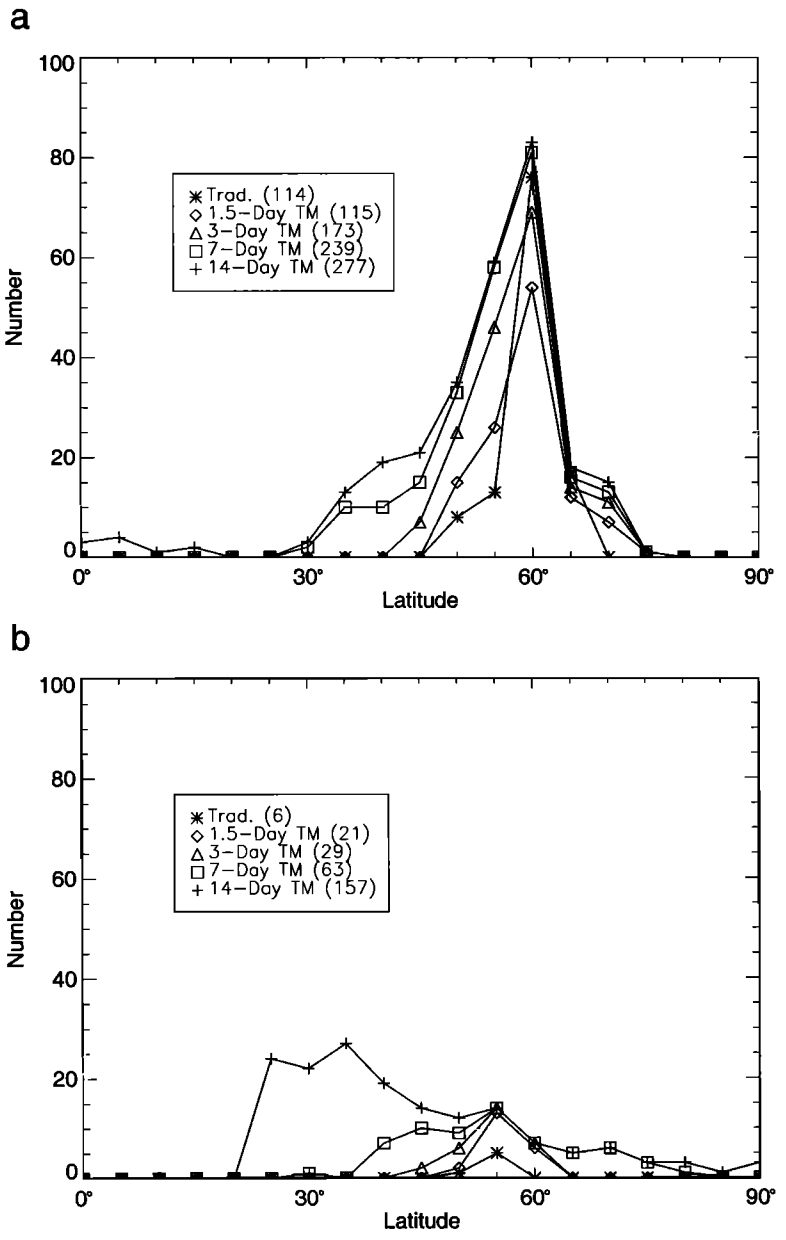

Figure 5. Distribution of coincidences occurring March 12 through April 5, 1995 at 800 K using traditional criteria and the trajectory-mapping approach as a function of latitude: (a) Northern Hemisphere and (b) Southern Hemisphere. Note that the trajectory approach greatly expands both the number of coincidences and the latitude range over which they occur.

ally necessitate the use of zonal means to produce meaningful comparisons.

2.3.2. Traditional approaches: Zonal mean comparisons. Figures 6a and 7a show the standard zonal mean ozone profiles from HALOE and SAGE II for the 64°–66°N and 29°–35°S latitude bands, respectively, in which both instruments make measurements during the period March 18–20, 1995. Each zonal mean consists of 45 sunset profiles. Figures 6b and 7b show the corresponding percent differences between the HALOE and SAGE II observations The traditional results correspond to the lines connected by the squares (□). The agreement between the two data sets appears quite good (to within 5%), particularly above 18 km. Disagreements lower down may be due to the presence of aerosols.

Traditional techniques identify real differences between the observed HALOE and SAGE II ozone data, for reasons yet to be entirely determined. Nevertheless, the traditional techniques leave something to be desired. In order to build-up enough coincidences to be statistically meaningful, traditional techniques must either use relaxed temporal and spatial criteria or combine a substantial number of months of SAGE II and HALOE data. In the former case, local meteorology can significantly affect the validation. In the latter case, seasonal and annual variations and trends in the data could skew the analysis.

The importance of determining the cause of the discrepancy and which of the two measurements is correct is clear: much current research involves the determination of ozone trends with an accuracy of the order of a percent or two per decade [e.g., *Stolar-*

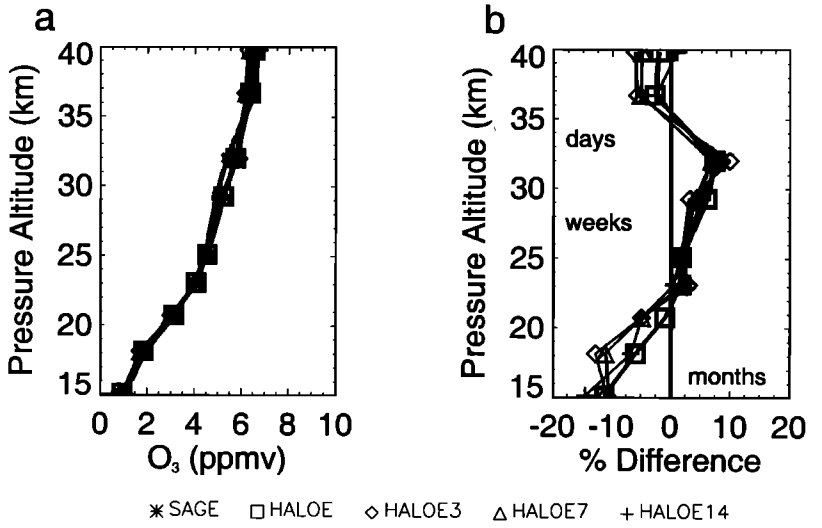

Figure 6. HALOE versus SAGE II ozone in the Northern Hemisphere for March 19, 1995: (a) Zonal mean profiles between 400 and 1200 K (15–40 km) using traditional (HALOE) and trajectory-mapping (TM) coincidence criteria. For the trajectory case, 3-day (HALOE3), 7-day (HALOE7), and 14-day (HALOE14) calculations are shown. (b) Percent differences between the HALOE and SAGE II zonal mean ozone profiles and the approximate photochemical lifetime of odd oxygen as a function of altitude.

ski et al., 1991; *Hollandsworth et al.*, 1995]. We must therefore have a similarly precise estimate of the accuracy of the measurements that go into these trend calculations.

2.3.3. Trajectory–Mapping Approach. Plate 1 shows a synoptic trajectory map of the HALOE measurements on the 800 K potential temperature surface for 1200 UT on March 19, 1995. To produce this map, the model advects 4 weeks of HALOE data (March 5 to April 2) with a combination of forward and backward trajectory calculations using balanced winds calcuated from the National Centers for Environmental Prediction (NCEP) meteorological analyses [*Randel*, 1987; *Newman et al.*, 1988]. The use of both forward and backward trajectories tends to minimize the impact of errors incurred in the passive advection scheme used in isentropic trajectory calculations due to diabatic or photochemical effects (see section 4.1). Each HALOE measurement is initialized in the model as a tightly packed cluster of five parcels (small dots in Plate 1) and advected to 1200 UT on March 19. Superimposed on the map are the SAGE II observations (large triangles) gathered on March 19. We consider those HALOE parcels within 400 km (see section 4.2 for a discussion of the sensitivity of our results to this choice) of and observed within 1.5 days of the SAGE II measurements to be coincident. As shown in the work of *Morris et al.* [1995], the advection of parcels over short time periods (like 1.5 days) should not lead to substantial errors. Notice that by using TM, we substantially enhance the coverage provided by the HALOE data as compared to that which results from 1 day of solar occultation observations (e.g., the SAGE II data that appear as triangles in Plate 1).

Figure 8 shows a scatterplot of coincident, 1.5-day, trajectory-mapped HALOE averages versus the individual SAGE II observations for the March 1995 period. First, we notice an increase in the number of coincidences as compared to those found in Figure 4 (the longer the trajectory calculations, the larger the increases, as shown in Table 2). The increased number is due, in part, to the

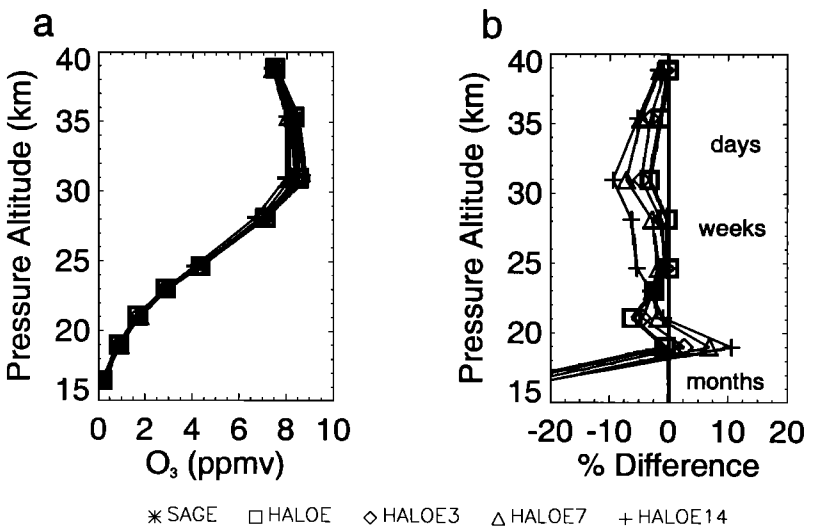

Figure 7. Same as Figure 6 but for the Southern Hemisphere.

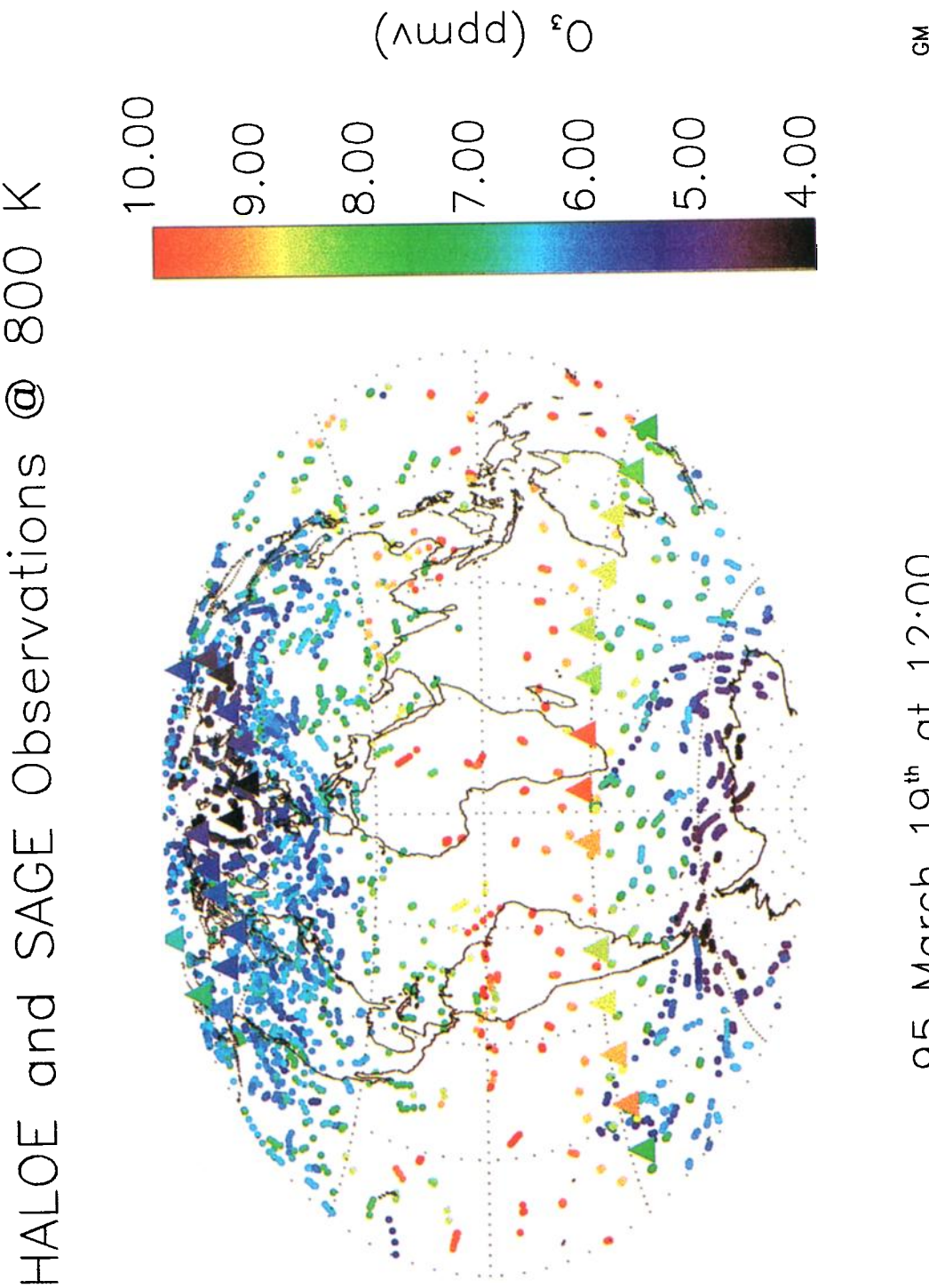

Plate 1. Synoptic trajectory map at 1200 UT on March 19, 1995, of HALOE observations (small dots) made between March 5 and April 2 on the 800 K potential temperature surface (~30 km). SAGE II observations (large triangles) from March 19 are overplotted.

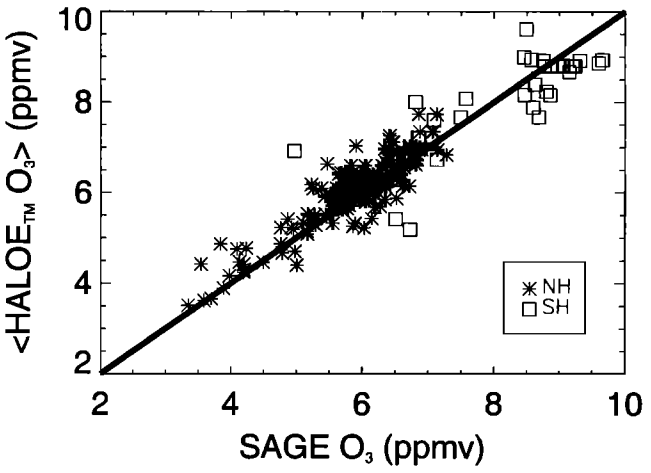

Figure 8. HALOE versus SAGE II during the period February 26 through April 19, 1995, using trajectory-mapping (TM) approach. Trajectory calculations are limited to a 1.5-day duration. Advected HALOE measurements within 400 km of the SAGE II observations are considered coincident. Comparisons are done using ozone data gathered on the 800 K potential temperature surface (~30 km). NH indicates coincidences in the Northern Hemisphere, while SH indicates coincidences in the Southern Hemisphere. Compared with Figure 4, the TM approach yields substantially more coincidences than the traditional approach.

fact that we are no longer restricted to the latitude bands of coincidence. The trajectory technique permits the comparison of measurements outside those latitude bands. Figure 5 shows the latitude distribution of the coincident measurements as a function of the maximum trajectory advection duration. As discussed in section 2.3.1, the starred line shows the distribution of traditional coincidences. Notice that the traditional coincidences are confined to the narrow latitude bands of overlap (one in the Northern Hemisphere and one in the Southern Hemisphere) between the observations of the two instruments. Using TM, we substantially expand the latitudes of intercomparison, so that using 14-day calculations, we provide comparisons at essentially all latitudes from 70°S to 80°N. We can therefore comment on the agreement between HALOE and SAGE II at latitudes outside those at which they concurrently measure.

Further, the impact of the technique on the uncertainty of our comparisons is small if not beneficial. Table 2 lists the standard correlation coefficients r and RMS differences between HALOE and SAGE II ozone observations on the 800 K surface during the March 1995 time period as computed using traditional and trajectory-mapping approaches. We define the correlation coefficient to be

$$r=\frac{\sum_{i=1}^{N}(x_i-\bar{x})(y_i-\bar{y})}{\sqrt{\left(\sum_{i=1}^{N}(x_i-\bar{x})^2\right)\left(\sum_{i=1}^{N}(y_i-\bar{y})^2\right)}},$$

where the x_i are the trajectory-mapped average of HALOE measurements near SAGE II observations, $\bar{x}$ is the mean of the x_i, y_i are the SAGE II observations, and $\bar{y}$ is the mean of the y_i. Notice that the RMS errors associated with trajectory advection periods of up to a 7-day duration are actually smaller than those found using the traditional coincident comparison technique. This behavior is due at least in part to the asynoptic nature of the traditional comparisons. In order to produce more than eight coincidences over the 6-week study period, we were forced to employ a 12-hour temporal coincidence criteria. During March 1995 at 800 K (~10 hPa or ~30 km), mean wind speeds from NCEP are 18–20 m/s (or 68–72 km/hr). Over the course of the 12 hours between HALOE and SAGE observations, the HALOE observation will move an average of around 800 km. Such distances are twice our correlation circle radius of 400 km, which suggests that the instruments may frequently make their measurements in entirely different air masses. The TM approach takes into account the dynamical motion occurring in the atmosphere between the time of the two measurements, thereby reducing the meteorological component of the observed variance. The observed increase in RMS errors for the 14-day trajectory calculations above traditional coincident RMS errors is consistent with known diabatic timescales over which the isentropic calculations used in this analysis become unreliable [e.g., *Morris et al.*, 1995].

To further examine the effect of our trajectory calculations on the uncertainty of our comparisons, we extend our analysis vertically to include nine levels between 400 and 1200 K (15–40 km). At each level we examine zonal means of the SAGE II and HALOE data from March 18–20, 1995, when the two instruments are observing at the same latitudes in both the Northern Hemisphere (64°–66°N) and the Southern Hemisphere (29°–35°S). Figures 6a (Northern Hemisphere) and 7a (Southern Hemisphere) show zonal mean profiles of the raw HALOE and SAGE II data as well as the 3-day, 7-day, and 14-day trajectory-mapped data from 1200 UT on March 19, 1995. Figures 6b and 7b show the percent difference between HALOE and SAGE II ozone measurements as given by

$$\%\ \text{difference} = 100 \times \frac{(\text{HALOE}-\text{SAGE II})}{\text{SAGE II}}.$$

Again, the two raw zonal mean profiles generally agree to within 5% throughout the profile in both hemispheres. Both the Northern Hemisphere (winter) and the Southern Hemisphere (summer) studies indicate that the 3-day case is virtually indistinguishable from the raw zonal mean comparison above 20 km. The 7-day case shows less than a 7% difference throughout the profile, even in the winter hemisphere, while the14-day case still shows less than a 10% difference. Between 18 and 25 km, where the lifetime of ozone is long, the trajectory method appears to result in differences of less than 5% as compared to the standard zonal mean results.

Figure 7b shows a clear trend in the Southern Hemisphere ozone profile shape with increasing integration periods: the longer the integration time, the farther away from the simple zonal mean the trajectory-mapped profile becomes. Furthermore,

Table 2. Correlation and Root-Mean-Square Statistics and Number of Coincidences in the Southern Hemisphere and Northern Hemisphere for HALOE–SAGE II Intercomparisons

Method	r	RMS, %	SH	NH
Traditional	0.87	10.4	6	145
1.5-day TM	0.93	8.0	31	156
3-day TM	0.90	8.4	58	247
7-day TM	0.84	10.0	146	437
14-day TM	0.80	12 2	337	601

See text for definition of RMS statistics. TM indicates trajectory-mapping approach. All comparisons are performed on the 800 K potential temperature surface. HALOE, Halogen Occultation Experiment; SAGE II, Stratospheric Aerosol and Gas Experiment II.

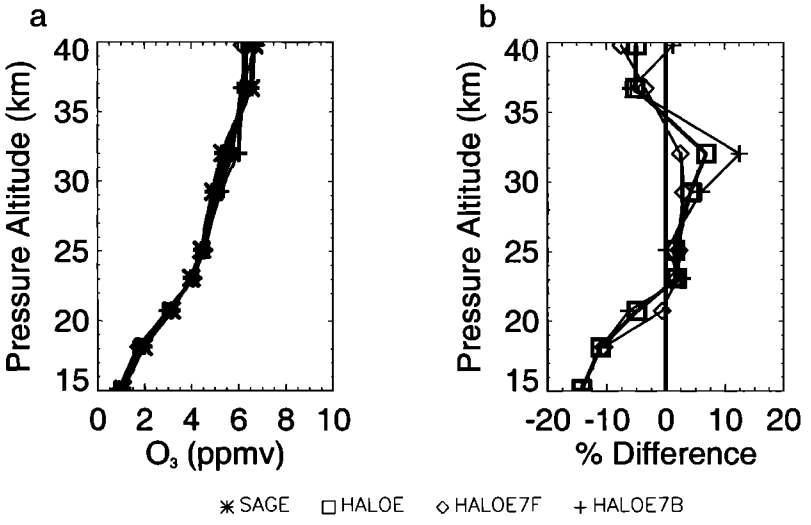

Figure 9. Comparison of zonal mean, trajectory mapped HALOE ozone profiles using 7-day forward only (◇), 7-day backward only (+), and 7-day combined (□) trajectory calculations. (a) Zonal mean profiles. (b) Percent difference between HALOE and SAGE II

the disagreement of the trajectory-mapped HALOE data with SAGE II observations becomes more negative at the altitude of the peak in the ozone mixing ratio profile (~30 km) and more positive below the peak. The neglect of diabatic processes and photochemistry in our analysis, particularly at the higher altitudes, is responsible for part of the increased uncertainty. TM is therefore best used in regions where the constituent lifetime is long and the magnitude of the diabatic circulation is relatively small. Both conditions are better satisfied below 27 km.

Finally, Figure 9 shows the impact of only using either forward or backward trajectory calculations. Here, we examine the effect on the zonal mean of the 7-day trajectory-mapped HALOE ozone data in the Northern Hemisphere on March 19. The "◊" line represents the zonal mean profile calculated from forward-only trajectories, the "+" line represents the zonal mean determined from backward only trajectories, and the "□" line represents the combined trajectory approach. In Figure 7b, we show the percent differences between the TM HALOE and SAGE II observations relative to SAGE II. Biases are clearly introduced when unidirectional trajectory calculations are employed: forward-only calculations tend to preserve mixing ratios longer than is warranted. In regions of descending air motion, the biases result in ozone values too high above the ozone peak and too low below it. The reverse is true for the backward-only calculations. As Figure 9 demonstrates, the biases of the forward- and backward-only calculations tend to offset one another. The combination of forward and backward trajectories therefore minimizes the biases and approximately doubles the number of parcels available to construct trajectory maps compared with either the forward or backward calculations alone. These results are supported by the sensitivity study using MLS water vapor described in section 4.1.

2.4. Case Study 3: HALOE Versus Ozonesondes

As a further demonstration of the validity of TM, we compare satellite ozone data from HALOE with ozonesondes. Figure 10 shows a comparison of ozone profiles derived from trajectory-mapped HALOE data (constructed as described in section 2.3.3) with those observed by ozonesondes. The composite sonde profiles are constructed from an average of ozonesonde observations at five nearby European stations: Hohenpeissenberg (48°N, 11°E), Legionowo (52°N, 21°E), Lindenberg (52°N, 14°E), Payerne (47°N, 7°E), and Praha (50°N, 15°E). Gridded ozone fields are produced for 1200 UT (the same time as the sonde measurements) on March 22 and April 5, 1995, from the trajectory-mapped HALOE data using a Barnes scheme. The gridded maps are then interpolated to the sonde locations and averaged over the same five stations. Note that we have not had to create zonal mean HALOE or SAGE II data for comparison with the sondes, a process that would have eliminated real longitudinal structure in the satellite data fields. The profiles show remarkably good agreement from 400 K (~15 km) to 800 K (~30 km).

3. Precision Assessment: The Problem of Evaluating Data From a Single Instrument

In assessing satellite data precision, previous efforts have relied upon an analysis of output from retrieval codes, observed data variability in the tropics, and comparison of measurements made near the same location on consecutive orbits. While the first approach produces estimates for every measurement, it does not incorporate any information external to the specific retrieval of interest to substantiate its conclusions. The latter two approaches are discussed in detail in the UARS Validation Special Issue of the Journal of Geophysical Research (1996). A brief review of these two techniques follows.

3.1. Previous Approaches

The Upper Atmosphere Research Satellite (UARS) orbits the Earth ~15 times each day at an altitude of 585 km in a plane inclined 57° with respect to the equator. The orbit precesses at a rate of 5° per day, providing coverage of all local times above a given geographic region about once every 36 days. The orbit permits the Microwave Limb Sounder (MLS) to observe latitudes between ~80° in one hemisphere and 34° in the other. Approximately every 36 days, UARS performs a yaw maneuver. This spacecraft maneuver is required to keep the instruments mounted on the "cold side" of the spacecraft in shade. The yaw maneuver effectively switches the primary hemisphere of study for the limb sounding instruments. The latitude bands that occur at the extreme limits of observation contain the highest spatial density of measurements.

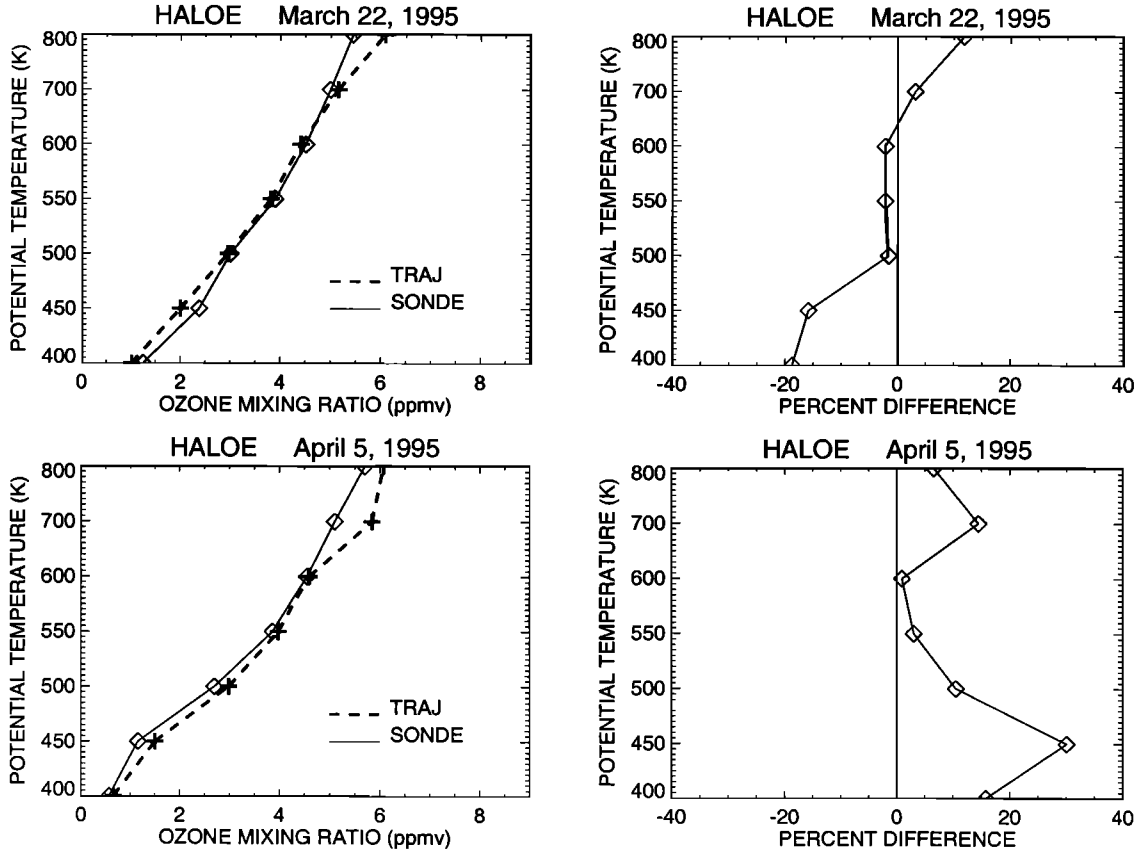

Figure 10. Comparison of ozone profiles constructed from trajectory-mapped HALOE data with a mean ozone profile from five European ozonesondes (see text for details).

Figure 11 shows the observation pattern of a single day of MLS measurements during a north looking UARS time period. Figure 12 shows a magnified view of a small region from 240° to 360° E and from 60° S to 10° N depicting the geographic overlap of two successive orbits. The close proximity of points both in space (less than 100 km) and in time (~1.6 hours) near the extreme latitudes of observation supports the assumption that such pairs of observations were made in the same air mass. Such data could then be used to empirically estimate instrument precision. These close coincidences only occur at the extreme latitudes of observation and thus only permit evaluation of measurement precision at two latitudes during each UARS period. The technique has been attributed to *Rodgers et al.* [1996], and a complete dis-

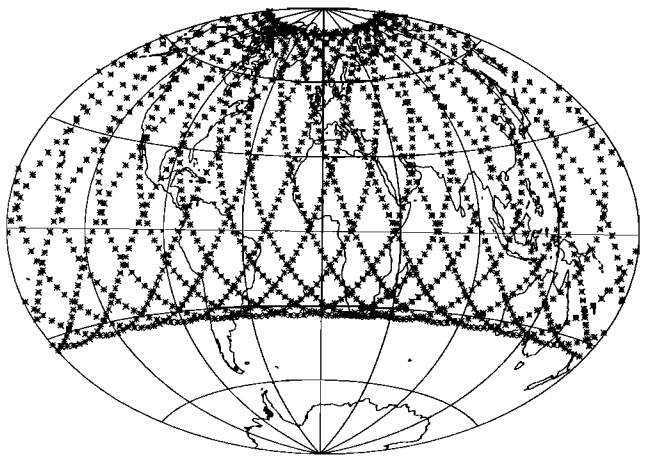

Figure 11. Map showing the typical observation pattern of MLS on a single day.

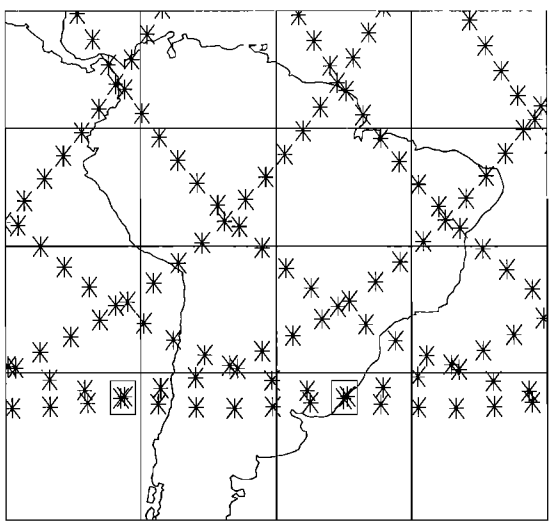

Figure 12. Close-up of the MLS observation pattern in central South America. Notice the two boxed regions that each contain a pair of MLS observations made within 96 min and 100 km of one another. Such observation pairs have been used to assess instrument precision.

cussion of the approach appears in the work of *Lahoz et al.* [1996].

The other approach for estimating precision examines the variability of tropical observations on a single day. Under the assumption that a tropical trace gas field in the stratosphere is relatively homogeneous, the variance of observations in a narrow tropical latitude band can be interpreted as an estimate of the precision of the observations. *Lahoz et al.* [1996] rely upon this technique to provide their estimates of single-profile precision for MLS water vapor, which range from 3 to 7%.

3.2. Trajectory-Mapping Approach

We now apply the trajectory-mapping technique to the problem of determining the precision of MLS water vapor data. We choose water vapor for its long lifetime in the middle to lower stratosphere, although in principle, the technique can be applied equally well to any dynamically conserved trace gas species. We examine water vapor retrievals during 10, 1-week-long periods between December 1991 and April 1993. Our analysis includes both hemispheres during the late winter/early spring season, the Northern Hemisphere in early winter, and the Southern Hemisphere in early summer.

3.3. Case Study 4: MLS Water Vapor Data

For this study we use Version 4 MLS water vapor data. Published validation of Version 3 MLS water vapor data suggests single-profile precision estimates of 3–7% for altitudes between 46 and 0.22 hPa [Lahoz et al., 1996]. Level 3 data are interpolated from the standard UARS pressure surfaces onto six isentropic surfaces between 550 and 1200 K using NCEP temperature data. Trajectory calculations are run adiabatically using the NCEP balanced winds.

We employ the TM technique to produce maps of the MLS water vapor field every 12 hours. The newest (± 6 hour) MLS observations are then compared to an average of the nearby, advected MLS observations. The technique used here is almost identical to that outlined earlier (section 2.1.3) with one exception: instead of comparing the new observations of one instrument to the advected observations of another, a single instrument provides the data for comparison against itself. We examine two statistics in the evaluation of the precision of the measurements: the RMS difference and the bias. The RMS error is defined as in section 2.2, and the bias is given by

$$\Delta=\frac{1}{N}\sum_{i=1}^{N}\frac{\bar{y}_i-x_i}{x_i},$$

where $\bar{y}_i$ are the averages of the trajectory-mapped MLS data near the newest MLS observation (x_i) and N is the total number of MLS observations that have trajectory-mapped coincidences. In general, we employ a combination of forward and backward trajectory calculations for several reasons. First, the use of the combination of forward and backward trajectories increases the density of data by utilizing observations made both before and after the time of interest. Second, isentropic calculations neglect diabatic effects, which, as noted earlier, can have a significant effect on air parcel motion in the stratosphere on a timescale of ~5–7 days [*Morris et al.*, 1995; *Schoeberl and Sparling*, 1994; *Sutton et al.*, 1994]. For example, *Manney et al.* (1995) found significant vertical motion of from 3–7 K/day decreases in potential temperature associated with episodes of low ozone in the northern midlatitudes. By including both forward and backward trajectory calculations, we minimize the impact of neglected diabatic processes. We investigate this hypothesis further in a sensitivity study described in section 4.1.

First, we calculate the precision of the MLS water vapor data using a traditional approach on data gathered during the period December 13–24, 1992. For the purposes of this case study, we define traditional coincidences in a manner similar to that of *Lahoz et al.* [1996] to be those MLS observations made on successive orbits near the turnaround points within 0.1 day and 100 km of each other. Under such circumstances, the two observations have overlapping fields of view. Figure 13 shows a scatterplot of such pairs of observations for the 800 K potential temperature surface (~30 km). As Figure 13 shows, the traditional approach demonstrates a good agreement between such pairs of measurements, with an RMS error of 4.3%. Over the 11-day time period the traditional approach yields 302 coincidences, all of which occur in the two narrow latitude bands at the extreme limits of the MLS geographic coverage: one near 80°N and one near 34°S.

We then repeat the analysis for five other potential temperature surfaces: 550, 600, 700, 1000, and 1200 K. On each level we calculate the zonal mean RMS statistic in each 1° latitude band. The results appear in Plate 2. As Plate 2 demonstrates, only the two, narrowly defined latitude bands contain traditionally defined coincidences. The traditional approach demonstrates a good agreement between the coincident MLS observation pairs, with RMS errors of less than 6% throughout the profiles at both latitudes.

We next apply the trajectory-mapping technique to the same data using 3-day trajectory calculations and a 400-km coincidence criterion. Figure 14 shows a scatterplot of the trajectory-mapped predictions versus the MLS observations for the 800 K level. We first notice substantially more coincidences (14,310) using the TM technique than found in Figure 13 using the traditional approach. The magnitude of the RMS error is 4.9%, slightly higher than that found using the traditional approach. Given the close proximity in time and space of the traditionally coincident pairs, this result is not surprising: we expect the traditional approach to perform at its best under such circumstances. The trajectory results, however, are not limited to two narrow latitude bands. The trajectory approach produces comparisons for nearly every MLS observation, regardless of its latitude. We also note from Figure 14 that the x variable shows more variance than

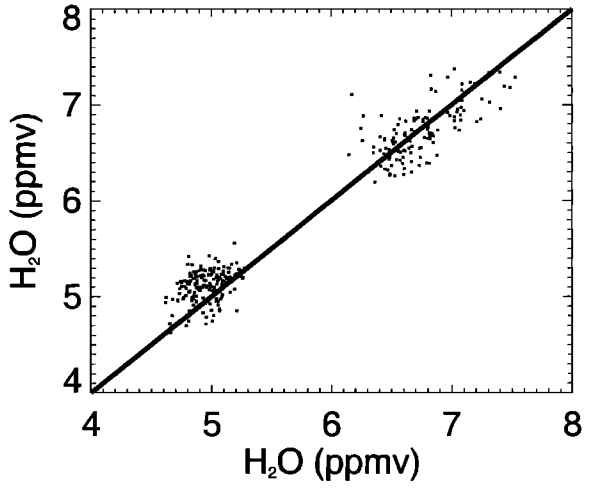

Figure 13. Scatterplot of coincident MLS water vapor observations on the 800 K potential temperature surface for the 11-day period of December 13–24, 1992 as determined using a traditional approach.

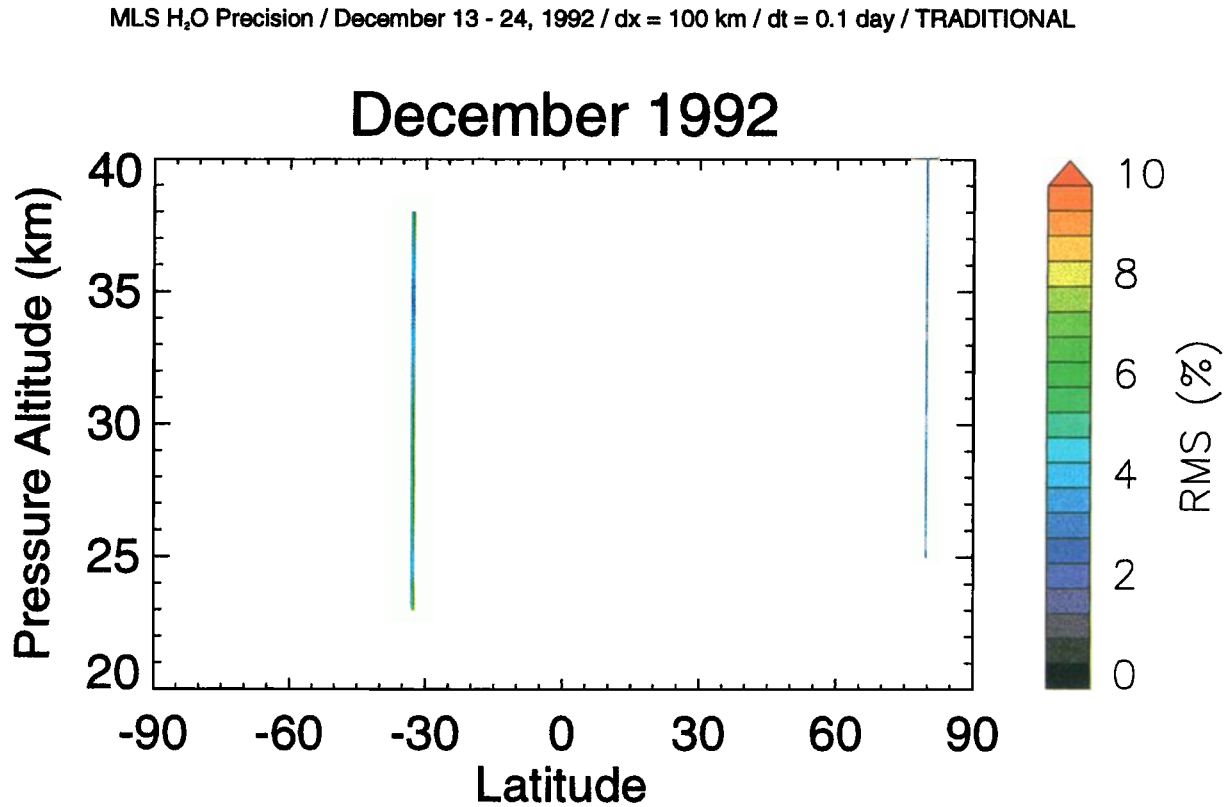

Plate 2. Zonal mean profiles of the root-mean-square difference between the MLS water vapor observation pairs noted in Figure 12 as determined using the traditional approach during the period December 13–24, 1992. Notice that such pairs occur in only two, narrowly defined latitude bands at the geographic extrema of the observations.

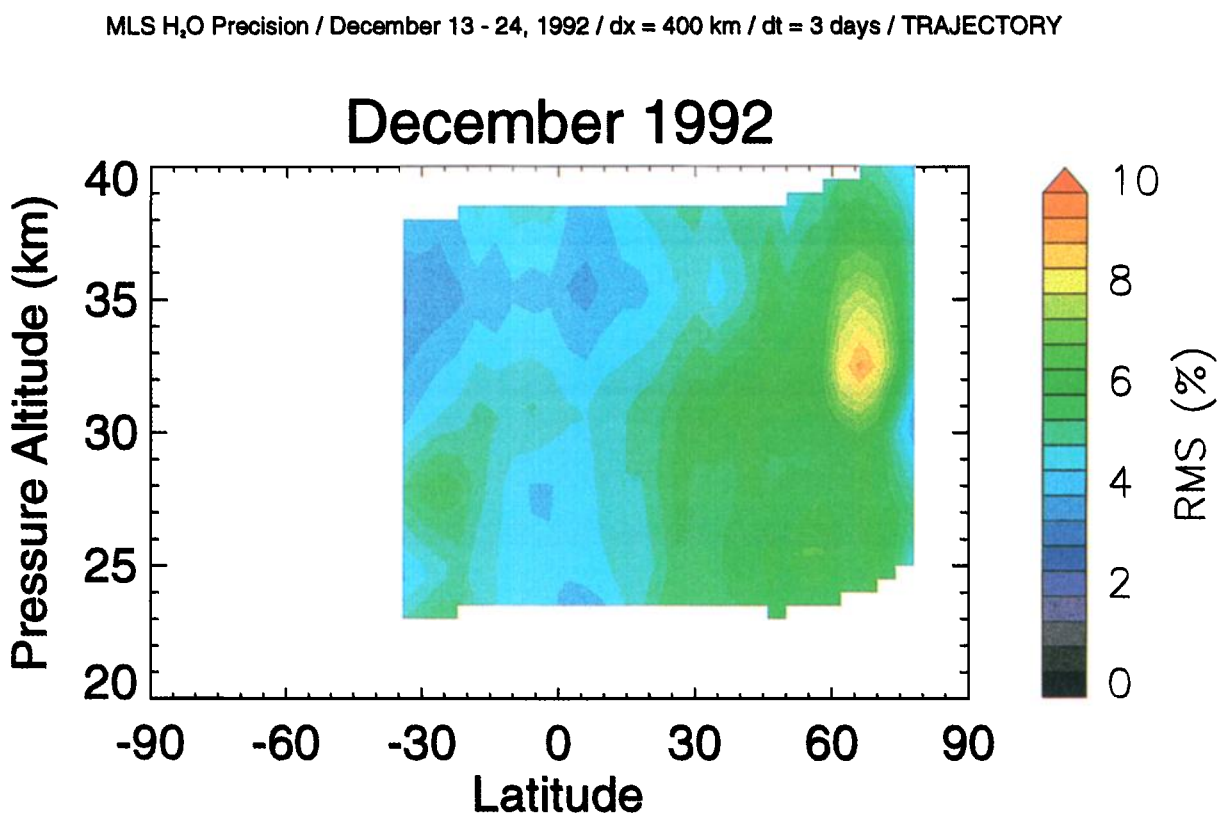

Plate 3. Zonal mean cross section of the root-mean-square difference between trajectory-mapped MLS water vapor data and new observations during the period December 13–24, 1992. Trajectory mapping produces estimates of measurement precision at all observed latitudes.

the y variable does. This effect can be attributed to the fact that the y variable represents an average of observations nearby the observation that appears as the x variable data point. As a result, outliers are more likely to appear in the x variable than in the y variable, owing to the effect of averaging on the latter.

As with the traditional case, we then repeat the TM analysis for the other five potential temperature surfaces. On each level we calculate the zonal mean RMS statistic in 5° latitude bands. The results are shown in Plate 3. Even a cursory examination of Plates 2 and 3 reveals that the trajectory-mapping technique greatly expands the latitude range over which estimates of data precision can be made as compared to the traditional approach. The trajectory results indicate data precision of the order of 3.5–6% in the tropics and fairly consistent 6% estimates through the midlatitudes. The highest precision uncertainties are found near 60°N and 33-km altitude, with values near 9%. The location of this region closely coincides with the latitude and altitude of the polar night jet core during this time period. The relatively large magnitude of the RMS statistic in this region is probably a result of the dynamics, which create a region of very strong gradients in both the wind fields and the trace gas constituents. We might expect that shorter trajectory calculations or smaller correlation distances would reduce the RMS statistic. Sensitivity studies of both of these quantities (not shown), however, demonstrate very limited effects on the results in this case. We therefore conclude that the assumption that both the trajectory-mapped and new observations occur in the same air mass is breaking down. Real geophysical variability is responsible for the observed increase in the precision statistic. In this case the precision statistic must be interpreted as consisting of both a random error component and a component representing the variability present in the real atmosphere.

Plots similar to Plate 3 can be produced using the TM technique for other seasons as well. The summer/fall hemisphere (not shown) is characterized by precision uncertainties of 3–6%, with low values at high latitudes, low latitudes, and high altitudes. The winter/spring hemisphere (not shown) is characterized by 4–7% precision uncertainties with locally higher levels near the polar night and subtropical jets.

4. Sensitivity Studies

Additional studies investigate a number of parameters in an attempt to establish the reliability of the TM technique and quantitatively evaluate the uncertainties introduced by the technique in its estimates of the precision uncertainty of the MLS water vapor data. Among the questions to be investigated are the following: What is the effect of changing the duration of the trajectories used in the construction of the trajectory maps? What is the effect of changing the geographic correlation criteria on the TM results? Are there any biases introduced by the trajectory technique? How do the results change if only forward trajectory calculations are used in the construction of the trajectory maps? How do the results vary from season to season? Are there hemispheric differences? We will attempt to address these questions in sections 4.1–4.3.

4.1. Sensitivity to the Trajectory Direction and Duration

We demonstrate the importance of using a combination of forward and backward trajectory calculations through a detailed examination of the long-duration TM study of December 1992. In this study, trajectory maps of MLS water vapor were produced using calculations of up to a 14-day duration. Again, traditional coincidences are defined to be those MLS observations made on successive orbits near the turnaround points within 0.1 day and 100 km of each other. Trajectory-mapped coincidences are defined to be those advected measurements that fall within a circle of radius 400 km around the new MLS observation. We examine two effects: the direction of the trajectory calculations (forward, backward, or both) and the duration of the trajectory calculations.

We first examine the effects of the duration of the trajectory calculations on the RMS and bias statistics for a 14-day, forward and backward combined trajectory run from December 1, 1992, to January 5, 1993. A week-long period in the middle (December 15–22, 1992) is used in the subsequent analysis. This week of results consists of 2-week trajectory calculations in both the forward and backward directions. The profiles are constructed from averages of all MLS data that meet both the traditional and trajectory coincidence criteria. (These data points occur only in the two narrow latitude bands near 80°N and 34°S in which the traditional coincidences occur.) A comparison of these profiles, which appears in Figure 15, therefore indicates the impact of the long-duration trajectory calculations on the results. The traditional approach is plotted as the solid line. The trajectory approach is shown for three different calculation durations: 3 days, 7 days, and 12 days. For the 12-day calculation, only trajectories of 10.5–13.5 days duration are included. Similarly, for the 7-day calculation, only trajectories of 5.5–8.5 days duration are included, and for the 3-day calculation, only trajectories of 1.5–4.5 days duration are included. Thus the profile corresponding to the 12-day trajectory calculation consists of coincidences of new MLS observations with observations that have been advected forward or backward in the trajectory model for 10.5–13.5 days. Over such long periods of time, the accumulated errors due to uncertainties in the wind fields and diabatic effects, which have been ignored in our isentropic calculations, become important, resulting in the observed increase in the RMS statistic seen in Figure 15a. Nevertheless, Figure 15b suggests that a combination of forward and backward calculations results in a bias that does not change with time. We test this hypothesis more thoroughly below.

In addition, Figure 15b suggests that the biases introduced by the trajectory calculations in this study are less than 0.5%, on average, throughout the profile. The apparent lack of bias in the trajectory results may be explained as follows. Under the assumption that diabatic effects act to change the local mixing ratio of a trace gas species roughly linearly over short periods of time, the inclusion of both "future" and "past" data in trajectory maps (through a combination of backward and forward trajectory calculations, respectively) acts to minimize the bias inherent in the

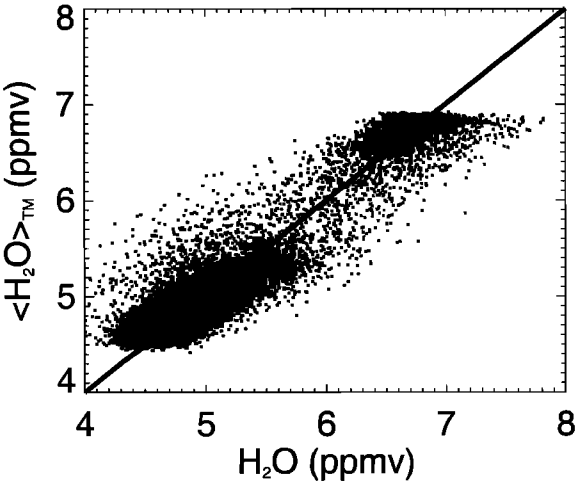

Figure 14. As in Figure 13 except here we apply the trajectory-mapping technique.

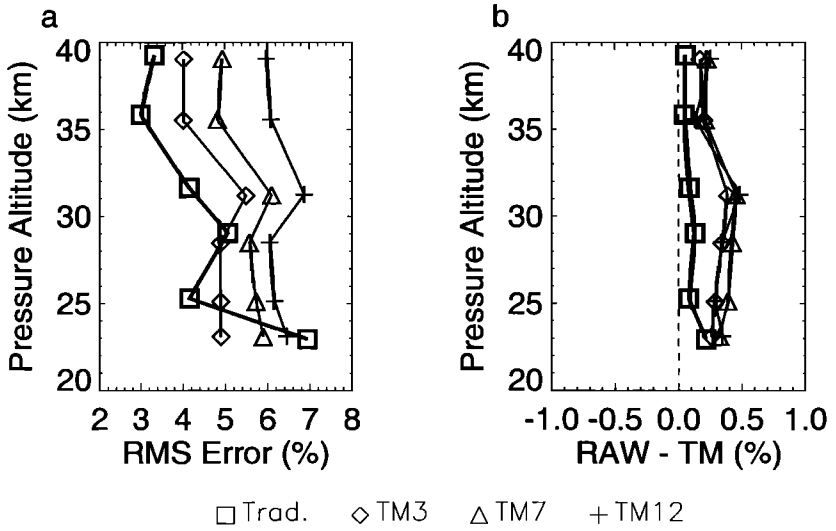

Figure 15. Comparison of (a) the root-mean-square and (b) the bias statistics (see text) between the traditional approach and the trajectory-mapping (TM) approach using calculations of 3 (TM3), 7 (TM7), and 12 (TM12) ± 1.5 days for the week-long study period of December 15–22, 1992. The trajectory results use a combination of forward and backward calculations. None of the biases are statistically significantly different from zero.

isentropic assumption. Errors that accumulate in the forward trajectory calculations are offset by errors that accumulate in the backward calculations. Trajectory maps constructed with both forward and backward calculations therefore provide a fairly accurate reflection of the present distribution of a trace gas species in the atmosphere.

The effect of the neglected diabatic heating is reflected in the RMS statistic, however, which increases steadily with the duration of the trajectory calculations, as can be seen in Figure 15a. The 3-day trajectory results show ~1% higher RMS differences than the traditional results, while the 7-day trajectory results show ~2% higher, and the 12-day trajectory results show ~2.5–3% higher RMS differences throughout the profile. The magnitude of the error introduced by the duration of the isentropic trajectory calculations will clearly be a function of the vertical gradient of the trace gas species being mapped and the strength of the diabatic heating at the time and location of the analysis. The numerical results from this study therefore should not be considered to represent the magnitude of the error introduced by all trajectory calculations of such duration during all seasons. Furthermore, the data in Figure 15 reflect the errors incurred by using only calculations of a particular duration. In general, trajectory maps are not constructed in the manner outlined above. Instead, a 7-day trajectory map consists of trajectory calculations of lengths 0–7 days instead of only calculations of 5.5–8.5 days. Therefore the results of Figure 15 provide an upper limit to the errors inherent in a typical 7-day trajectory map of MLS water vapor.

The difference between the typical application (described above) and that presented in Figure 15 can be seen in the results of another sensitivity study, shown in Figure 16. Here the results are separated into the two latitude bands in which traditional coincidences occur. Figure 16a demonstrates that near the southern subtropical barrier the trajectory results are consistently better than the traditional approach throughout the profile, while Figure 16b shows that at high northern latitudes the RMS statistic for trajectory approach is less than 1% different from the traditional approach throughout the profile. In general, the trajectory results are consistent with and often better than the traditional approach in assessing instrument precision, even at places and times when the traditional approach works very well. The TM technique, however, has a significant advantage over the traditional approach in its far broader scope of geographic coverage.

Many studies using trajectory techniques have applied unidirectional isentropic calculations. This approach is inherently flawed owing to the nonconserved nature of the advected trace gas as well as to the neglected diabatic effects. Here, we illustrate an important advantage gained by using bidirectional trajectory calculations. Figure 17 shows the RMS and bias statistics for the unidirectional forward- and backward-only calculations corresponding to the long-term study of December 1992 presented in Figure 15 and discussed above. Again, the solid "*" line represents the traditional results, while the other lines represent the trajectory results ("+" for 3-day TM, "◊" for 7-day TM, and "Δ" for 12-day TM). We note that both the forward only (solid lines) and backward only (dashed lines) trajectory calculations introduce RMS errors of nearly the same magnitude for calculations of the same duration. The biases, however, tend to be in opposite directions between the two unidirectional calculations as compared to the combined results shown in Figure 15.

This result is consistent with the fact that our isentropic trajectory calculations neglected diabatic effects. Outside of the tropics, forward-only trajectories neglect the descent of air relatively rich in water vapor, resulting in a low bias compared to the actual observations. Conversely, backward-only trajectories result in a high bias compared to the actual observations. By using a combination of forward and backward trajectory calculations, we successfully counter the impact of the uncertainties introduced in the long, unidirectional trajectory calculations, as hypothesized earlier. A similar argument can be made for the accumulation of numerical errors over time within the trajectory model as well. Studies using the isentropic RDF technique with unidirectional trajectory calculations may therefore incur a bias in the mapped constituent field due to neglected chemical and diabatic effects.

4.2. Sensitivity to Correlation Distance

One important parameter in TM is the separation distance between two measurements that are assumed to be correlated. Historically, correlation distances have ranged from a few meters

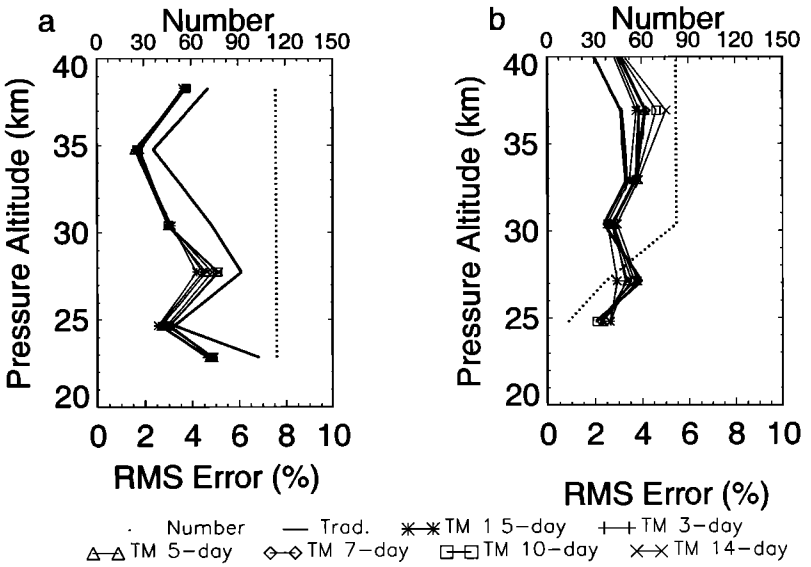

Figure 16. Zonal mean plots of the average root-mean-square (RMS) error statistic (see text) for the period December 15–22, 1992, as determined using traditional and trajectory-mapping approaches. Trajectory calculation durations of 1.5, 3, 5, 7, 10, and 14 days are shown by the thin lines. The traditional results are indicated by the thick line. (a) The RMS profile near the southern subtropical boundary (~30°S) Upper Atmosphere Research Satellite (UARS) turnaround. (b) The RMS profile at the high northern latitude (~80°N) UARS turnaround. The dotted line indicates the number of coincidences achieved with the 14-day trajectory-mapping technique.

in the Balloon Ozone Intercomparison Campaign [*Hilsenrath et al.*, 1986] to 1000 km or more for validation of HALOE [*Park et al.*, 1996] and SAGE II data [*Veiga et al.*, 1995]. Larger correlation distances tend to increase the number of coincident measurements (which acts to decrease the RMS statistic), but they also increase the variance (which acts to increase the RMS statistic) owing to the inclusion of pairs of observations that are, in fact, made in different air masses. In TM a similar trade-off exists between correlation distance and uncertainty.

Figure 18 summarizes the sensitivity of the RMS statistic to correlation distance under all conditions. Data from 10, 7- to 11-day study periods have been compiled to construct Figure 18. These 10 periods are December 13–24, 1991; January 29–February 7, 1992; March 4–15, 1992; April 11–21, 1992; September 4–15, 1992; October 4–15, 1992; December 13–24, 1992; January 18–29, 1993; March 4–15, 1993; and April 4–13, 1993. Again, only those coincidences found using both the traditional and trajectory techniques are included in the analysis, thereby restricting the results to those four narrow latitude bands in which the traditional approach produces coincidences: ~80°S, ~34°S, ~34°N, and ~80°N. These restrictions on the comparisons produce the most favorable results possible using the traditional approach. Again, by comparing our TM results with the traditional results in these cases, we can effectively estimate the magnitude of the uncertainty associated with the TM technique itself. The 3-day trajectory calculations were used in all five cases testing the sensitivity of the trajectory results to correlation circle size.

Figure 18 indicates that in general, the largest and smallest correlation distances result in the largest RMS differences. Cor-

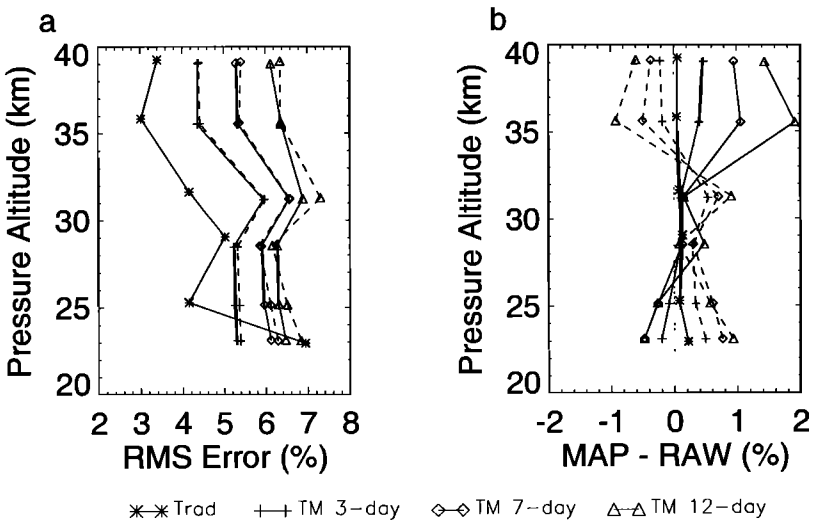

Figure 17. As in Figure 15 but with forward-only (solid lines) and backward-only (dashed lines) trajectory calculations plotted separately. (a) Root-mean-square statistic. (b) Bias statistic. See text for definitions.

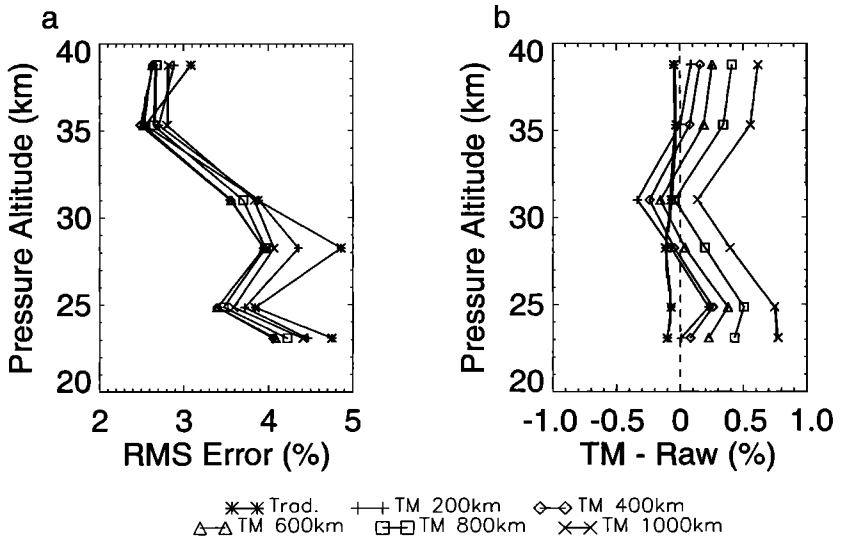

Figure 18. Comparison of the root-mean-square and bias statistics between the traditional and trajectory approach using correlation distances of 200, 400, 600, 800, and 1000 km. (a) Root-mean-square statistic. (b) Bias statistic. See text for definitions. As in Figure 15, none of the biases are statistically significantly different from zero.

relation circles with radii of 400 or 600 km seem to consistently produce the smallest RMS differences throughout the profile. A similar study by *Rex et al.* [1998] revealed that the best results in their validation of ozonesonde observations using trajectory calculations occurred for coincident pairs with separation distances of less than 400 km, supporting the results obtained here. Below 30 km the trajectory approach appears to produce smaller RMS differences than the traditional approach does regardless of the correlation distance. Between 30 and 35 km, trajectory results are comparable to the traditional approach. Near 38 km the trajectory results again show improvement compared to the traditional approach. While some seasonal and latitudinal dependence can be seen in the data, the 400-km correlation criterion is not found to increase the RMS statistic by more than 1% as compared to other correlation distances in any season at any altitude.

Although there appears to be a systematic drift toward negative biases with larger correlation circle sizes in Figure 18, neither the drift nor the bias profiles themselves are statistically significant (standard deviations of the bias range from 3 to 6%, an order of magnitude larger than the bias itself). Furthermore, we have no reason to expect such a systematic trend in the bias with larger correlation distances, nor should we expect such a trend to be observed in other constituents. These results essentially demonstrate that nowhere in the profile between 22 and 40 km is a

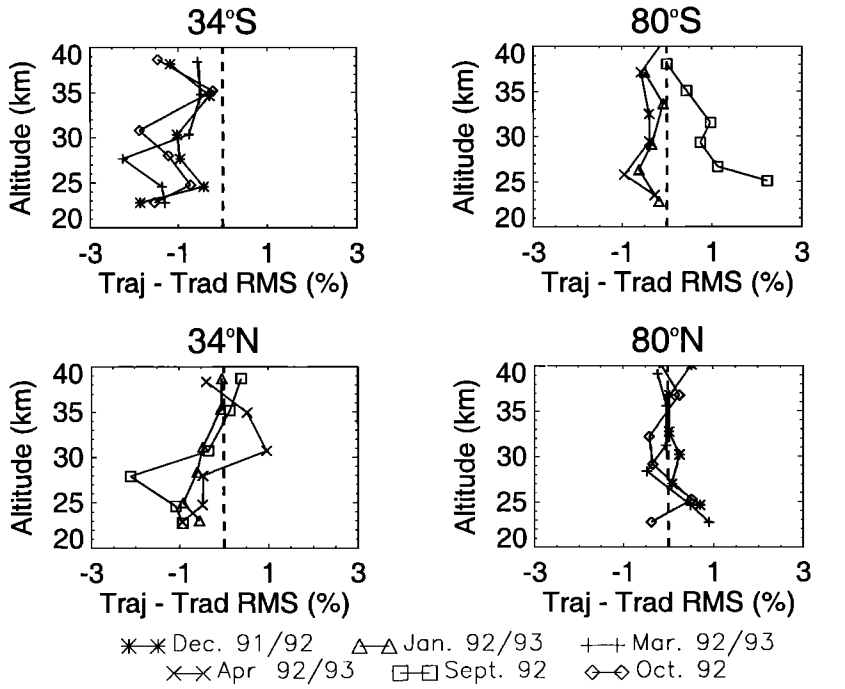

Figure 19. Comparison of the 3-day trajectory mapping root-mean-square precision against that derived using the traditional approach in the four latitude bands in which the traditional approach can be applied. See text for details.

statistically significant bias introduced by the 3-day trajectory calculations in large-scale studies covering all seasons.

We observe a common quality to the RMS profiles depicted in Figures 15, 17, and 18: relative maxima near 23 and 28 km and relative minima near 25 and 35 km. Version 4 MLS water vapor data are retrieved only on every other UARS pressure level, which implies that the actual MLS data are found near 22, 27, 32, 38, and 43 km. Data at other UARS levels result from a linear interpolation of the adjacent levels. In our study we apply a cubic spline to the data to derive the MLS water vapor at the isentropic levels used in this study. The fact that the minima appear farther from the actual retrieved levels than the maxima suggests that our interpolation scheme is not responsible for the relative maxima in the RMS profiles. In fact, it is likely that our interpolation scheme has acted to reduce errors inherent in the retrievals themselves and that the actual errors may be somewhat larger than those represented here.. Version 5 MLS water vapor data, which recently have been released, provide MLS data on all the UARS pressure levels. The new data should lead to improved vertical interpolation between levels and probably better overall results.

4.3. Sensitivity to Geographic Location and Season

The quality of the TM results depends upon the quality of the meteorological analyses. The impact of the choice of meteorological analysis has been investigated by *Morris* [1994]. However, a detailed discussion of the impact of the meteorological analyses on the trajectory results is beyond the scope of this work. A future paper will examine this issue and a methodology for applying TM to evaluating the quality of the wind field analyses. Previous work, however, indicates that while individual trajectories may diverge quite rapidly between model runs using different wind field analyses, an ensemble of trajectories maintains the same gradients in an advected trace gas field for long periods of time [*Morris et al.*, 1995]. We therefore expect our results to be generally applicable to trajectory calculations regardless of the wind field analysis employed. Particular dynamical events may be better captured by one wind field analysis than another, in which case the selection of the wind field analysis input into the trajectory model may affect the results. The optimal choice of wind field analysis for any individual event must be determined on a case-by-case basis.

To evaluate the performance of the TM technique as a function of latitude and season, we again use the MLS water vapor data and restrict our analysis to those latitudes and times when the traditional approach produces coincidences. Figure 19 summarizes the results of our comparison in each of the four latitude bands in which traditional coincidences occur. Plotted in Figure 19 is the difference between the RMS statistic for the MLS observations as determined with the TM technique and that determined with a traditional approach. Negative values indicate smaller RMS values for the trajectory technique than for the traditional approach. The lines for January, March, and April represent average results from the two, 1-week study periods in 1992 and 1993. The line for December represents the average results of the two, 1-week study periods in 1991 and 1992. The lines for September and October represent the results from the lone, 1-week study period in 1992. The trajectory results employ 3-day calculations and a 400-km correlation circle radius.

Figure 19 demonstrates that the TM technique provides a consistent improvement in the subtropics throughout the profile compared to the traditional technique, with the possible exception of the northern subtropics in spring near 30 km. At high southern latitudes the TM technique appears to be comparable to the traditional approach in the summer and fall seasons, although somewhat worse than the traditional approach in September. The explanation for this result probably lies in the quality of the wind field analyses: the sparse nature of the meteorological data that provide input for the meteorological analyses in the Southern Hemisphere results in larger wind field uncertainties. The fact that TM yields somewhat larger RMS errors as compared to the traditional approach in this case is therefore not surprising.

At high northern latitudes the trajectory results are consistent with results from the traditional approach throughout the profile. While the meteorological data in the Northern Hemisphere are more densely sampled than those in the Southern Hemisphere, the dynamics in the Northern Hemisphere are much more active. Larger diabatic descent rates and sharper gradients in the constituent and wind fields are found in the Northern Hemisphere than are found in its southern counterpart. These factors can lead to large uncertainties in the isentropic trajectory calculations. Nevertheless, the results of our study of MLS water vapor indicate that the TM technique produces results consistent with the traditional approach in those latitude bands where both techniques can be successfully applied. Again, it is important to keep in mind that we have compared the trajectory results to the results from the traditional approach at times and locations favorable to the latter technique. The results therefore represent a worst case scenario for the performance of the trajectory technique against the traditional approach. The trajectory technique is capable of producing results at times and places inaccessible to the traditional approach, as best demonstrated by Plates 2 and 3.

5. Summary and Conclusions

We have applied the TM technique with good results in several case studies and examined the sensitivity of the results yielded by the technique to a variety of parameters. TM proved effective in the comparison of one sparse data set with one dense satellite data set (HALOE and MLS ozone), the comparison of two sparse data sets (HALOE and SAGE II ozone), the comparison of satellite data with balloons (HALOE versus ozonesondes), and the establishment of instrument precision using a single data set (MLS water vapor). Taking advantage of dynamical information, TM has allowed us to improve and expand our comparisons beyond the brief periods and narrow latitude bands of overlap that usually restrict traditional techniques.

In the MLS-HALOE comparison study the TM approach increased the number of coincidences and greatly expanded the range of latitudes at which coincidences occurred as compared to the traditional approach. Of particular importance, these advantages were achieved without a corresponding significant increase in the uncertainty of the comparisons. The TM results compare favorably with results achieved using traditional approaches in a study designed so that the traditional approaches would perform well. The 1.5-day trajectories showed less than 1% differences in the RMS statistic as compared with those found using a traditional approach. These results enhance our confidence in the results achieved by the trajectory-mapping technique in studies where the traditional approaches do not generally perform well.

We next applied the TM technique to the comparison of two sparse data sets. The TM technique showed significant advantages over the traditional approach in the comparison of ozone data from SAGE II and HALOE. The TM technique substantially increased the number of coincidences while often decreasing the uncertainty as compared to the traditional coincidence approach. The latter effect can be attributed to the fact that TM accounts for the dynamical motion between the observation times, which traditional approaches have previously ignored. Even the 14-day trajectory calculations, for which we know the diabatic effects cause significant departures from isentropic trajectories, did not appear to significantly increase the uncertainty of the comparisons. The technique works best below 27 km, where the lifetime

of ozone is fairly long and the magnitude of the diabatic circulation is relatively small. In this region of the lower stratosphere, the assumptions of the conservation of ozone and potential temperature along the calculated trajectories work best.

Comparison of zonal means of the trajectory-mapped HALOE data to traditionally calculated SAGE II zonal mean data demonstrated that the trajectory technique has little negative impact. Unlike the traditional zonal means, however, the trajectory technique preserves longitudinal structure in the ozone field that is lost in zonal averaging validation. Comparison of the trajectory-mapped data with ozonesondes also showed good agreement, further establishing the ability of TM to validate variability in constituent fields on a regional scale.

We applied TM to the problem of determining the precision of the MLS water vapor data set. The MLS observation pattern provides coverage with a relatively high density of observations. In two latitude bands near the geographic limits of observation, the MLS measurements on successive orbits occur within 96 min and 100 km of one another, making the application of a traditional comparison technique highly successful. We compared results obtained using the TM approach to data within the same narrowly defined latitude bands. In these latitude bands our analysis demonstrated that the trajectory results are generally consistent with the traditional approach. Only in the high-latitude, Southern Hemisphere, low-altitude, winter case does the trajectory approach yield higher RMS errors than the traditional approach does. Considering that such tests have been performed under a best-case scenario for the traditional technique, the TM approach performs impressively well. The major advantage of the TM technique over the traditional technique is that we can ascertain the precision uncertainty of the MLS data over the entire latitude range in which the observations are made, unlike the traditional approach that is restricted to only those latitude bands where coincidences occur.

Results from a number of sensitivity studies permit us to optimize our technique as well as to quantify the related uncertainties. We investigate the sensitivity of our trajectory results to several important parameters: the duration and direction (forward or backward) of integration of trajectories, the maximum distance between trajectory-mapped measurements considered to be coincident, and the latitude and season of the trajectory calculations.

Forward-only and backward-only trajectory calculations introduce biases, owing to diabatic motions (which are neglected in isentropic trajectory calculations) and photochemical changes in species concentration. By applying a combination of forward and backward trajectory calculations, the uncertainties of longer trajectory calculations can be minimized. The longer the duration of the trajectory calculations, the greater the uncertainty introduced in the RMS statistic. The bias statistic in bidirectional trajectory calculations, however, does not appear to increase with the trajectory duration. We therefore recommend the use of a combination of forward and backward trajectories for all isentropic trajectory-mapping calculations. The use of unidirectional isentropic calculations can produce significant errors on relatively short timescales, owing to neglected chemical and diabatic effects.

A variety of correlation distances were tested for altitudes between 20 and 40 km under a wide range of geographic and seasonal conditions. Under most circumstances the 400-km correlation distance resulted in the smallest RMS errors. While some variation exists in the results as a function of altitude, latitude, and season, under no circumstance did the 400-km correlation distance produce an RMS statistic with a magnitude more than 1% greater than the smallest RMS statistic associated with some other correlation distance. We therefore recommend, in general, a 400-km correlation distance with data sets such as the MLS water vapor data.

We also conclude that while the shorter-duration trajectory calculations generally produce results with smaller precision uncertainties, longer-duration calculations (of up to 14 days) do not necessarily result in substantial increases in precision uncertainty estimates. In fact, only at high latitudes in the winter season do the longest trajectory calculations seem to significantly increase uncertainty estimates. The temporal breadth of our analysis allows us to conclude that the trajectory approach is as good as if not better than the traditional approach throughout the year with the exception of September in the Southern Hemisphere. These same studies suggest that the increased number of correlated observations gained through the use of longer trajectory calculations offsets the increased uncertainty introduced through longer modeled advection periods. Our sensitivity studies help establish the magnitude of the uncertainties introduced by the TM technique itself as well as the conditions under which the application of the technique is most appropriate.

Our study provides confidence in the application of the TM technique to data validation at latitudes beyond those at which the traditional technique can be successfully applied. The TM technique can thereby provide reliable estimates of measurement accuracy and precision for entire data sets rather than relying upon extrapolation of results achieved through the validation of a small subset of the data through traditional techniques. TM is a powerful, reliable tool for data validation studies.

Acknowledgments. The research presented in this paper has been supported through a number of grants: the Department of Energy Graduate Fellowships for Global Change administered by the Oak Ridge Institute for Science and Education, a National Research Council/NASA Goddard Space Flight Center Post-Doctoral Fellowship, the UARS Guest Investigator program, and the EOS Validation program through grant number NAG5-8490. Thanks to the entire MLS team for the water vapor data product, to the SAGE II team for its ozone data product, and to the HALOE team for its ozone data product

References

Bailey, P.L., et al., Comparison of cryogenic limb array etalon spectrometer (CLAES) ozone observations with correlative measurements, *J. Geophys. Res., 101*, 9737–9756, 1996

Conner, B.J., J Scheuer, D.A Chu, J.J. Remedios, R.G Grainger, C.D. Rodgers, and F.W. Taylor, Ozone in the middle atmosphere as measured by the improved stratospheric and mesospheric sounder, *J. Geophys. Res., 101*, 9831–9841, 1996.

Cunnold, D.M., H. Wang, W.P. Chu, and L. Froidevaux, Comparisons between Stratospheric Aerosol and Gas Experiment II and Microwave Limb Sounder ozone measurements and aliasing of SAGE II ozone trends in the lower stratosphere, *J. Geophys. Res., 101*, 10,061–10,075, 1996

Froidevaux, L., et al , Validation of UARS Microwave Limb Sounder ozone measurements, *J Geophys Res., 101*, 10,017–10,060, 1996.

Gille, J.C., et al., Accuracy and precision of cryogenic limb array etalon spectrometer (CLAES) temperature retrievals, *J. Geophys Res., 101*, 9583–9601, 1996.

Hilsenrath, E. et al., Results from the Balloon Ozone Intercomparison Campaign (BOIC), *J. Geophys. Res , 91*, 13,137–13,152, 1986.

Hilsenrath, E., D E Williams, R.T. Caffrey, R.P. Cebula, and S.J. Hynes, Calibration and radiometric stability of the Shuttle Solar Backscatter Ultraviolet (SSBUV) experiment, *Metrologia, 30*, 243–248, 1993.

Hollandsworth, S.M., R.D. McPeters, L.E. Flynn, W. Planet, A.J. Miller, and S Chandra, Ozone trends deduced from combined Nimbus–7 SBUV and NOAA 11 SBUV/2 data, *Geophys. Res. Lett., 22*, 905–908, 1995.

Kawa, S.R., et al., Interpretation of NO_x/NO_y observations from AASE-II using a model of chemistry along trajectories, *Geophys. Res. Lett., 20*, 2507–2510, 1993.

Kumer, J B , et al., Comparison of correlative data with HNO_3 version 7 from the CLAES instrument deployed on the NASA Upper Atmosphere Research Satellite, *J. Geophys. Res., 101*, 9621–9656, 1996

Lahoz, W.A., et al., Validation of UARS microwave limb sounder 183 GHz H_2O measurements, *J. Geophys. Res., 101*, 10,129-10,149, 1996.

Lopez–Valverde, M.A., et al., Validation of measurements of carbon monoxide from the improved stratospheric and mesospheric sounder, *J. Geophys. Res., 101*, 9929–9955, 1996.

Manney, G.L., R.W. Zurek, L. Froidevaux, and J.W. Waters, Evidence for Arctic ozone depletion in late February and early March 1994, *Geophys. Res. Lett., 22*, 2941–2944, 1995.

McDermid, I S., et al., Comparison of ozone profiles from ground-based lidar, electrochemical concentration cell balloon sonde, ROCOZ-A rocket ozonesonde, and stratospheric aerosol and gas experiment satellite measurements, *J. Geophys. Res., 95*, 10,037–10,042, 1990.

Morris, G.A., A demonstration and evaluation of trajectory mapping, Ph.D. thesis, Rice Univ., Houston, Tex., 1994.

Morris, G. A., et al., Trajectory mapping and applications to data from the Upper Atmosphere Research Satellite, *J. Geophys. Res., 100*, 16,491–16,505, 1995.

Morris, G.A., S.R. Kawa, A.R. Douglass, M.R. Schoeberl, L. Froidevaux, and J. Waters, Low-ozone pockets explained, *J. Geophys. Res., 103*, 3599–3610, 1998.

Newman, P.A., and M.R. Schoeberl, A reinterpretation of the data from the NASA stratosphere troposphere exchange project, *Geophys. Res. Lett., 22*, 2501–2504, 1995.

Newman, P.A., D.J. Lamich, M. Gelman, M.R. Schoeberl, W. Baker, and A.J. Krueger, Meteorological atlas of the southern hemisphere lower stratosphere for August and September 1987, *NASA Tech. Memo., 4049*, 1988.

Nightingale, R.W., et al., Global CFC measurements by UARS cryogenic limb array etalon spectrometer: Validation by correlative data and a model, *J. Geophys. Res., 101*, 9711–9736, 1996.

Park, J.H., et al., Validation of Halogen Occultation Experiment CH_4 measurements from the UARS, *J. Geophys. Res., 101*, 10,183–10,203, 1996

Pierce, R.B., W.L. Grose, and J.M. Russell, III, Evolution of Southern Hemisphere air masses observed by HALOE, *Geophys. Res. Lett , 21*, 213–216, 1994.

Randel, W.J., The evolution of winds from geopotential height data in the stratosphere, *J. Atmos. Sci., 44*, 3097–3120, 1987.

Remedios, J.J., et al., Measurements of methane and nitrous oxide distributions by the improved stratospheric and mesospheric sounder: Retrieval and validation, *J. Geophys. Res., 101*, 9843–9871, 1996.

Rex, M., et al., In situ measurements of stratospheric ozone depletion rates in the Arctic winter 1991/1992: A Lagrangian approach, *J. Geophys. Res., 103*, 5843–5853, 1998.

Rind, D., et al , Overview of the Stratospheric Aerosol and Gas Experiment II water vapor observations. Method, validation, and data characteristics, *J. Geophys. Res., 98*, 4835–4856, 1993.

Roche, A.E., J.B. Kumer, J.L Mergenthaler, G.A. Ely, W.G. Uplinger, J F. Potter, T.C. James, and L.W. Sterritt, The Cryogenic Limb Array Etalon Spectrometer (CLAES) on UARS: Experiment description and performance, *J. Geophys. Res., 98*, 10,763–10,775, 1993.

Roche, A.E., et al., Validation of CH_4 and N_2O measurements by the cryogenic limb array etalon spectrometer instrument on the Upper Atmosphere Research Satellite, *J. Geophys. Res., 101*, 9679–9710, 1996.

Rodgers, C.D., R.J. Wells, R.G. Grainger, and F.W. Taylor, Improved stratospheric and mesospheric sounder validation: General approach and in-flight radiometric calibration, *J. Geophys. Res., 101*, 9775–9793, 1996.

Russell, J. M., et al., The halogen occultation experiment, *J. Geophys. Res., 98*, 10,777–10,797, 1993.

Russell, J.M., et al., Validation of hydrogen chloride measurements made by the Halogen Occultation Experiment from the UARS platform, *J. Geophys. Res., 101*, 10,151–10,162, 1996a.

Russell, J.M , et al., Validation of hydrogen fluoride measurements made by the Halogen Occultation Experiment from the UARS platform, *J. Geophys. Res., 101*, 10,163–10,174, 1996b.

Schoeberl, M.R., and P. Newman, A multiple-level trajectory analysis of vortex filaments, J. Geophys. Res., *100*, 25,801-25815, 1995.

Schoeberl, M.R., and L. Sparling, Trajectory modeling, in *Proceedings of the International School of Physics: Diagnostic Tools in Atmospheric Physics*, edited by G.F.A.G. Visconti, Elsevier Science Publishing Company, Inc., New York, 1994.

Singh, U.N., et al., Stratospheric temperature measurements by two collocated NDSC lidars during UARS validation campaign, *J. Geophys Res., 101*, 10,287–10,297, 1996.

Stolarski, R.S., P. Bloomfield, R.D. McPeters, and J R. Herman, Total ozone trends deduced from NIMBUS 7 TOMS data, *Geophys. Res. Lett., 18*, 1015–1018, 1991.

Sutton, R.T., H. Maclean, R. Swinbank, A. O'Neill, and F.W. Taylor, High-resolution stratospheric tracer fields estimated from satellite observations using Lagrangian trajectory calculations, *J. Atmos. Sci., 51*, 2995–3005, 1994.

Taylor, F.W., Pressure Modulator Radiometry in *Spectrometric Techniques*, vol. 3, p. 137–197, Academic, San Diego, Calif., 1983.

Taylor, F.W., et al., Remote sensing of atmospheric structure and composition by pressure modulator radiometry from space: The ISAMS experiment on UARS, *J. Geophys. Res., 98*, 10,799–10,814, 1993.

Veiga, R.E., D.M. Cunnold, W.P. Chu, and M.P McCormick, Stratospheric Aerosol and Gas Experiments I and II comparisons with ozonesondes, *J. Geophys. Res., 100*, 9073–9090, 1995.

J. Gleason, M. R. Schoeberl, and J. R. Ziemke, Mail Code 916, NASA Goddard Space Flight Center, Greenbelt, MD 20771.

G.A. Morris, Dept. of Physics and Astronomy, Valparaiso University, Valparaiso, IN 46383. (Gary.Morris@valpo.edu)

(Received June 8, 1999; revised November 3, 1999;
accepted November 8, 1999.)